SOLVENT EFFECTS ON THE THERMAL AND SPECTROSCOPIC PROPERTIES OF POLY(2-METHOXY-5-(2'-ETHYLHEXYLOXY)-1,4-PHENYLENE VINYLENE) (MEH-PPV) THIN FILMS

by

PAUL REMENTER

A thesis submitted to the

Graduate School-Camden

Rutgers, The State University of New Jersey

In partial fulfillment of the requirements

For the degree of Master of Science

Graduate Program in Chemistry

Written under the direction of

Professor Georgia Arbuckle-Keil, Ph.D.

And approved by

_____

Georgia A. Arbuckle-Keil

_____

Alex J. Roche

_____

Luke A. Burke

Camden, New Jersey

October 2014

ABSTRACT OF THE THESIS

SOLVENT EFFECTS ON THE THERMAL AND SPECTROSCOPIC PROPERTIES OF POLY(2-METHOXY-5-(2'-ETHYLHEXYLOXY)-1,4-PHENYLENE VINYLENE) (MEH-PPV) THIN FILMS

By PAUL REMENTER

Thesis Director:
Professor Georgia A. Arbuckle-Keil

In 1990, Poly (phenylene vinylene) (PPV) became the first conjugated polymer used in polymer electroluminescent devices.[6] With the addition of alkoxy side chains, the PPV derivative poly(2-methoxy-5-(2'-ethylhexyloxy)-1,4-phenylene vinylene) (MEH-PPV) was able to be processed in many common organic solvents. However, it soon became apparent that the conditions under which MEH-PPV devices and thin films were prepared had a great effect on their morphology and electronic properties. Most notably, the choice of solvent used, whether aromatic or aliphatic, had the greatest effect on these properties.

Many research groups have studied the effects of different solvents and processing conditions on fluorescence, absorption and device operation. Very little research has been conducted however on how these different morphologies affect the thermal and mechanical properties of the thin films.

A differential scanning calorimeter (DSC), thermogravimetric analyzer (TGA) and differential mechanical analyzer (DMA) were used to observe the correlation between solvent choice and casting conditions on the thermal and mechanical properties of MEH-PPV thin films. Infrared spectroscopy (IR) was used to verify the quality of the cast films, as well as look for any shifts in the absorbance bands that changes in the morphology or residual solvents would create. Lastly, a spectrofluorophotometer was used to gain a better understanding of how the

emission band wavelengths are affected by factors such as solvent choice and conditions used for casting: under air atmosphere, under argon, in vacuum desiccators (under vacuum).

Acknowledgements

I would like to especially thank my research advisor Dr. Georgia A. Arbuckle-Keil, for her help, encouragement, insightful guidance, and tremendous patience.

Table of Contents

List of Figures

List of Tables

Chapter 1: Background Information on MEH-PPV

I. Introduction

Conjugated polymers combine the optoelectronic properties of semiconductors with the mechanical properties and processing advantages of plastics.[1] When functionalized with aliphatic side groups,[2] polymers often become soluble in organic solvents and can be solution processed at room temperature into large-area, optical-quality thin films.[3] These films can be easily processed into desired shapes that are useful in novel devices.[4] There is a potential for large cost-savings in applications that require visible band-gap semiconductors by using polymers over inorganic semiconductors.[5] Conjugated polymers therefore have potential uses in devices such as plastic light-emitting diodes (LED), [4, 6] photovoltaics,[7] transistors,[8-10] and newer applications such as flexible displays.[5]

The first conjugated polymer used in polymer electroluminescent devices was poly(p-phenylenevinylene) (PPV) in 1990.[6] However, PPV is insoluble in many organic solvents. With the addition of alkoxy side chains, the PPV derivative poly(2-methoxy-5-(2'-ethylhexyloxy)-1,4-phenylene vinylene) (MEH-PPV) (Figure 1.1) can lower the oxidation potential and also improve the solubility remarkably.[11] Despite the ease in constructing conjugated polymer-based devices with MEH-PPV, optimizing the performance of such devices is complicated by its molecular nature.[12] The method by which the polymer is processed has a direct effect on the conformation of the polymer chains, and can alter the electronic properties of the resulting polymer film,[12] a reason so many researchers have produced varying and sometimes conflicting results.

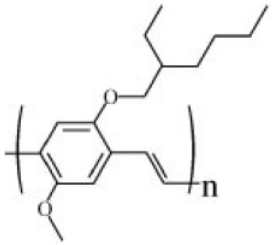

Figure 1.1: MEH-PPV repeat unit

II. Background Literature

A. Overview

There are several factors that can influence the formation of interchain species and aggregates in solutions of conjugated polymers: choice of solvent, molecular weight, polymer concentration, and nature of the side-chains on the polymer backbone.[13] These aggregates can persist through the casting process, and result in fundamental changes in the photophysical and electroluminescent behavior of conjugated polymer thin films.[13] When the π-electrons of two conjugated polymer chains overlap, significant electronic interactions between them can occur: this is one of the reasons film properties are sensitive to morphology.[13]

The formation of aggregates in solution can be controlled by the choice of solvent as well as the concentration, with better solvents promoting aggregation.[13, 14] These aggregate species are predominantly formed from conjugated segments on different chains, and have the ability to reduce luminescence efficiency.[5, 13]

Aromatic solvents such as chlorobenzene (CB) and toluene have a preferential interaction with the aromatic backbone of the polymer chain, and MEH-PPV will unfold in solution to maximize favorable π-π interactions between the polymer and the solvent, and thus the chains adopt a rigid, open conformation in solution.[13-15] With its more open conformation, CB and toluene provide a higher number of longer conjugation length segments than non-aromatics such as tetrahydrofuran (THF), chloroform (CF) and dichloromethane (DCM).[13, 15]

These longer segments promote aggregation as the concentration increases, with more segments available for interaction.[13]

Non-aromatic solvents such as THF, CF and DCM, have a preferential interaction with the aliphatic side chains of MEH-PPV.[15, 16] The polymer chains will coil tightly to maximize these interactions with the non-aromatic side groups and minimize interaction with the aromatic backbone.[13, 15, 16] These polymer coils create torsional defects along the backbone, which leads to shorter conjugation length and lower photoluminescence (PL) quantum yield.[13] The MEH-PPV chains do not coil in a way that allows significant π-electron interaction between chromophores on the same chain.[16] Aggregation can still occur, "*but only in high enough concentrations to force adjacent polymer coils together so that π-electron density is shared over a sufficient contiguous distance*."[16]

The conjugation length of the polymer changes in different solvents. In aromatic solvents such as chlorobenzene, there is a higher degree of interchain interaction. MEH-PPV LEDs based on films cast from CB have a higher injection current, lower turn-on voltage, and lower quantum efficiency than corresponding MEH-PPV devices fabricated with non-aromatic solvents (THF).[17] *"This illustrates an apparently fundamental trade-off when trying to optimize conjugated polymer films for maximum device performance: the same interchain interactions which promote charge transport are detrimental to luminescence efficiency."*[13, 17]

B. Solvent Influence on Device Properties

Aromatic solvents preferentially solvate the conjugated segments of MEH-PPV: this leads to a greater possibility of intimate contacts between conjugated groups and the metal atoms of devices (Figure 1.2).[18] Devices made with non-aromatic solvents have yielded smaller photo-currents, poorer polymer/anode contact, and lower electrical conduction than devices fabricated using aromatic solvents (similar film thickness).[18, 19] This is due to the different

molecular conformations in the polymer films. In non-aromatic solvents, there is a pronounced voltage lag between the injection voltage and light-emitting voltage (hole-injection voltage) as a result of the unbalanced charge injection. As an example, Ag/MEH-PPV/Ag devices show a smaller degree of asymmetry when MEH-PPV is processed from aromatic solvents.[18-20]

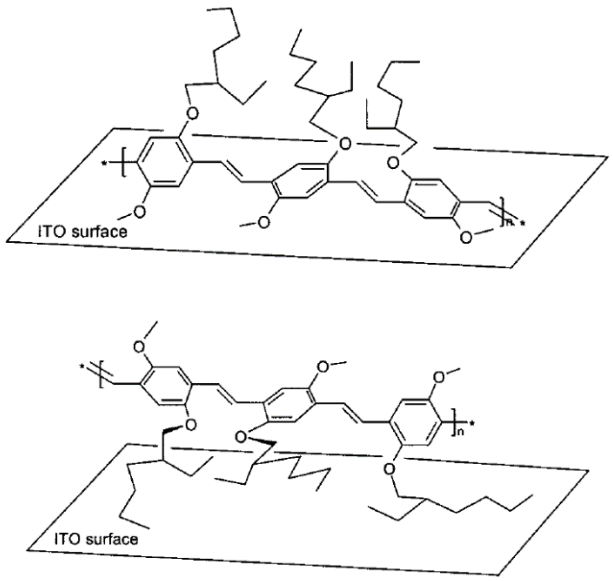

Figure 1.2: Non-aromatic solvents prefer to orient the non-aromatic side groups outside and "trap" the conjugated groups inside. Conjugated backbones are shielded by bulky alkyl side groups. This prevents intimate contacts between conduction groups.[18]

Nano-indentation results have shown that chloroform-cast MEH-PPV films have higher elastic modulus, hardness, and critical bending radius than toluene-cast films.[15] MEH-PPV forms tight coils when in non-aromatic solvent such as CF, and the higher mechanical properties could possibly be due to stronger intermolecular interactions and bonding which results in higher modulus. Toluene-cast films have a lower critical bending radius, which indicates they can bear a larger bending stress, which is useful for device fabrication.[15]

C. Crystallinity

In x-ray diffraction (XRD) scans, MEH-PPV films cast from THF exhibited a higher degree of anisotropy of chain orientation with respect to the substrate, as well as a higher degree of

crystallinity and larger crystalline domains than films cast from CB or p-xylene. The percentage of the benzene ring planes that are oriented in-plane for films cast from THF, p-xylene and CB are different. *"Better performance as a gain narrowing material is correlated with a higher degree of in-plane chain (backbone) orientation, with higher crystallinity, and with longer structural coherence lengths."*[21] Films cast from chloroform exhibit a lower degree of crystallinity than films cast from toluene.[22]

III. Film Production and Storage

A. Various Methods of Film Preparation

The extensive literature on MEH-PPV documents that the way in which MEH-PPV films are prepared has a dramatic effect on their morphology and resulting luminescence. Many researchers have tried to control the conditions under which the films are made.

The memory of the solution-phase conformation of MEH-PPV is retained through the casting process. Spin-casting of films allows for rapid evaporation of highly volatile solvents, yielding films which retain many of the characteristics of the solution. MEH-PPV in THF for example, forms a compact conformation (tight coils), and resists forming aggregates. When the solvent is rapidly evaporated in spin-casting, there is not enough time for the chain interactions to unfold into open conformations like in aromatic solvents, and the polymer chains will remain tightly coiled. These THF-cast films will have a relatively reduced amount of interchain aggregation compared to CB (aromatics).[13]

The thickness of MEH-PPV films is increased at lower spin-casting speeds, due to slower solvent evaporation from inside the polymer film. The lower spin speeds allow the polymer chains to have more time to relax into a more thermodynamically favorable conformation.[23]

"Methods which include spin casting at 4000-8000rpm or a low boiling point solvent should be excluded: these films have a meta-stable supramolecular structure which gradually changes." [24] Arnautov *et al.* prepared their samples by dissolving a measured quantity (0.5-2g/L) into solvent and stirring 60-90 minutes at 50°C. They employed both drop casting and slow-solvent evaporation onto substrates. The process in which solvent should be removed should be slow enough to permit macromolecules to form the optimal equilibrium and morphology.[24]

MEH-PPV chains are readily soluble in aromatic solvents such as xylene and chlorobenzene, and somewhat soluble in polar, nonaromatic organic solvents like tetrahydrofuran. By heating the polymer solution while stirring, Nguyen *et al.* found that the polymer fully solubilizes.[12] The processing, handling and storage of the cast films were carried out in an inert environment (i.e. nitrogen or argon-filled glove box).[12] Once cast, films should be dried for at least 24h at room temperature, suggests Yang *et al.*[21]

B. Importance of Film Storage

The storage of newly cast films is just as important as the casting process. Films are stored in the dark under inert atmosphere (N_2) or under vacuum to prevent photo-oxidation. [25]

Storing for 1 month in ambient, dark conditions, films became nearly isotropic with chains almost equally oriented parallel to and perpendicular to the plane of the film.[21] Results differ for samples stored under vacuum. Degradation rate, as measured by the anisotropic distribution of ordered benzene ring planes or the crystalline domains, is related to exposure to oxygen. [21]

C. Summary

There are many potential advantages for the use of MEH-PPV in today's high-tech devices. The ease of processing, mechanical and optoelectronic properties make it a cost-

effective alternative. The solvent used to dissolve MEH-PPV in solution, whether aromatic or aliphatic, can have a dramatic effect on the morphology and chain conformation of the polymer. These morphological differences can carry over into the films when cast. These differences have a direct effect on the optical and luminescent properties that make MEH-PPV so appealing.

While many research groups have studied the effects of different solvents and processing conditions on optical properties, luminescence and device operation, very little research has been conducted on how these different morphologies affect the thermal and mechanical properties of the thin films. These properties play significant roles in the stability and capacity of films in devices.

Chapter 2: Experimental: MEH-PPV Film Preparation and Storage

I. Overview

All dissolutions were tightly controlled by running an argon purge, heating and stirring for 24h under reflux for repeatability. Drop-casting of the polymer solutions is preferred over spin-casting to create films of consistency and uniform thickness. This is important when mounting onto the tensile jig during dynamic mechanical analysis. In order to try and simulate the rapid evaporation of spin-casting, films were cast into a vacuum desiccator to try and evaporate the solvent as quickly as possible (to "freeze" polymer chains in their solvent-induced form). To create the opposite effect (slow evaporation to allow polymer chains to relax and achieve a lower-energy state), films were cast in an argon glove bag to allow the solvent to slowly evaporate. As a control, films were prepared in a fume hood under normal room conditions. Once cast, all films were placed under vacuum to pull-off any remaining solvent, and stored in an argon glove box, in the dark, to prevent any oxidation or photo-degradation.

II. Dissolution

125.0 mg of the MEH-PPV powder [Sigma-Aldrich; M_n=70,000-100,000; Lot# MKBF2052V; Refrigerator stored] was weighed and added to a 100 mL round bottom flask. A magnetic stir bar was added, along with 25.0 mL of solvent. Chlorobenzene (CB) [Sigma-Aldrich Chromasolv for HPLC 99.9%], chloroform (CF) [EMD CX 1055-9 GR ACS Assay 99.8%], toluene (Tol) [Fisher Laboratory Grade] and dichloromethane (DCM) [Sigma-Aldrich ACS HPLC Grade 99.9%] were the solvents used in this study. The w/v ratio of the solution was 0.5%. The solution and flask were heated in a 50°C silicon oil bath while stirring. The solution was stirred with a reflux condenser attached (for low boiling point solvents) and a slow argon purge for a 24h period.

III. Casting

After 24h, the polymer-solvent solution was removed from the silicon oil bath to cool for ~5min, while still stirring under argon. Approximately 8 mL of the polymer solution was drawn into 3, 10 mL syringes. The polymer solutions were drop-cast into 60mm diameter polytetrafluoroethylene (PTFE) dishes, under 3 different conditions: these included an argon filled glove bag, a fume hood (normal atmosphere and room temperature) and a vacuum dessicator.

IV. Glove Bag

The polymer solution filled syringe was placed inside an argon-filled Glas-Col I^2R Glove Bag, along with a 60mm diameter PTFE dish, and Pyrex petri dish. An argon line was attached to the back of the glove bag, and the bag was purged 3 times to flush out oxygen. In the final purge, the bag was sealed 90% and the argon allowed to displace the remaining oxygen. The bag was then quickly sealed to minimize oxygen contamination. Once sealed, the polymer-solvent solution was carefully cast into the PTFE dish, which was sitting inside the Pyrex petri dish. This allowed the polymer solution in the PTFE dish to form an even film by keeping it parallel to the lab bench (Note: some oxygen would probably diffuse into the bag over time, as there was not a positive argon pressure throughout the solvent evaporation process. This is something to look into for future studies. While the argon atmosphere was one of the main focal points of this particular part of the experiment, the slower evaporation times compared to the vacuum desiccator and fume hood/ambient was also important). After a 24h period (longer for high boiling point solvents), the newly formed polymer film was removed from the PTFE dish, cut into 3 pieces (average thickness as measured by micrometer ~20 μm), and the Infra-red spectrum recorded. The films were then placed under vacuum and transferred to a Vacuum Atmospheres (VAC) Glove Box. Here they were stored in labeled zip-loc bags, in the dark.

V. Fume hood

Casting films in a fume hood allows them to dry under ambient conditions. A 60mm PTFE dish was placed on a marked position roughly in the center of the fume hood. Two wooden sticks were placed on each side of the dish. The polymer-solvent solution was cast into the PTFE dish. A glass jar was then placed over top of the PTFE dish, propped up slightly by the wooden sticks. This allowed for steady and consistent air flow over the solution-filled dish. After a 24h period, the newly formed polymer film was removed from the PTFE dish, cut into 3 pieces (average thickness as measured by micrometer ~20 μm), and the infra-red spectrum recorded. The films were then placed under vacuum and transferred to a Vacuum Atmospheres Dry Box. Here they were stored in labeled zip-loc bags, in the dark. These films will be referred to as being cast in "air."

VI. Vacuum desiccator

The fastest way to dry the polymer once drop-cast is by rapidly pulling the solvent off. This was done by casting the polymer-solvent solution into a 60mm PTFE dish that had been placed inside a small vacuum desiccator. Once the solution filled the PTFE dish, the lid was closed and the vacuum pump turned on to evacuate the desiccator. This process was conducted inside of a fume hood, with a cold-finger trap attached to collect the solvent. For the first 15min, the vacuum pressure on the dessicator was small: if the pressure was too great and the solvent allowed to evaporate too rapidly, the polymer solution would splatter and the consistency of the film affected. The films were held under vacuum for period of 4 hours, at which time they were removed from the PTFE dish. After removal, the newly formed polymer film was cut into 3 pieces (average thickness as measured by micrometer ~15 μm), and the infra-red spectrum recorded. The films were then placed under vacuum and transferred to a Vacuum Atmosphere Dry Box. Here they were stored in labeled zip-loc bags, in the dark.

Chapter 3: Thermal Analysis

I. Differential Scanning Calorimetry

A. Introduction

A differential scanning calorimeter, commonly referred to as a DSC, is one of the fundamental tools of thermal analysis. It measures the amount of heat that flows into and out of a sample as the temperature is changed, and can provide data that can be used to determine the glass (T_g) and phase transition temperatures (i.e. T_m, T_c).

By subjecting a sample material and reference standard to a change in temperature (±), changes in the heat capacity are observed as changes in heat flow. During a melting transition for example, when energy is needed to break the inter-chain bonds, heat flow will increase to the sample with respect to the reference. In contrast, heat is given off during crystallization, and heat flow to the sample will decrease with respect to the reference. By graphing these differences as a function of time and/or temperature, you can study the different changes a polymer (or any material for that matter) undergoes over a specific temperature range.

It has been well documented that changing the solvent and casting conditions by which MEH-PPV films are prepared result in different morphologies and degrees of aggregation.[12, 13, 16-21, 23, 24, 26-31] X-ray diffraction (XRD) scans have shown that this can affect crystalline domains and structure. [21] These altered morphologies and crystalline structure should be observable through DSC analysis, in the form of shifts in the glass transition temperatures and specific heat capacities. Since electroluminescent polymer films like MEH-PPV are used in devices which run current (LED) or operate under extreme conditions (Solar Cell), it is important to understand how these properties are affected by processing conditions.

B. Method

Samples were weighed on a Shimadzu AUW-220D analytical balance to 5.00±0.05 mg, and then hermetically sealed in 0.3MPa aluminum pans with a Shimadzu SSC-30 crimper. They were run on a Shimadzu DSC-60 with TAC-60L cooling accessory under the following conditions:

1. N_2 purge gas @ 30 mL/min (purge detector during testing)
2. N_2 dry gas @ 200 mL/min (purge electronics at low-temperature)
3. Isothermal Hold @ 0°C for 5 minutes
4. Ramp 20°C/min to 120°C
5. Isothermal Hold @ 120°C for 5 minutes

Each morning before testing, the DSC-60 was calibrated with Indium (T_m=156.63°C, c=28.45J/g) and Zinc (T_m=419.58°C, c=100.5J/g) in accordance with ASTM E967/968.

C. Glass Transition (T_g)

When the amorphous region of an amorphous or semi-crystalline material undergoes a reversible change from a hard (glass) to rubber-like state, it is known as the glass transition (T_g). During this transition, the heat capacity and thermal expansion coefficient change, and a shift in the DSC baseline is observed. This event is not a phase transition like T_m or T_c, but rather a relaxing of the inter-chain bonds. Many factors can vary the temperature at which this occurs, such as aging of the sample, oxidation, heating rate, purity, use of plasticizer, etc. Depending on the device and method in which the polymer is used, this information could be critical to efficiency and operability.

In order to observe this transition, a sample should be heated starting at ~50°C lower than the expected T_g. There are several ways in which to evaluate the T_g: some researchers use a specific point on the analysis curve, such as the onset, midpoint or peak temperature. Other

researchers use tangent lines to the transition peak. With both methods of analysis, results must be recorded and repeated in the same manner throughout the experiments, and the method of analysis clearly outlined. This ensures accurate and repeatable results.

For comparison, the glass transition temperatures in this study were calculated two ways; first, as the peak of the transition curve (Figure 3.1), and second as the intersection of the two tangents of the curve peak (Figure 3.2). Literature values for the glass transition temperature of MEH-PPV range from 60-70°C.[22, 32-34]

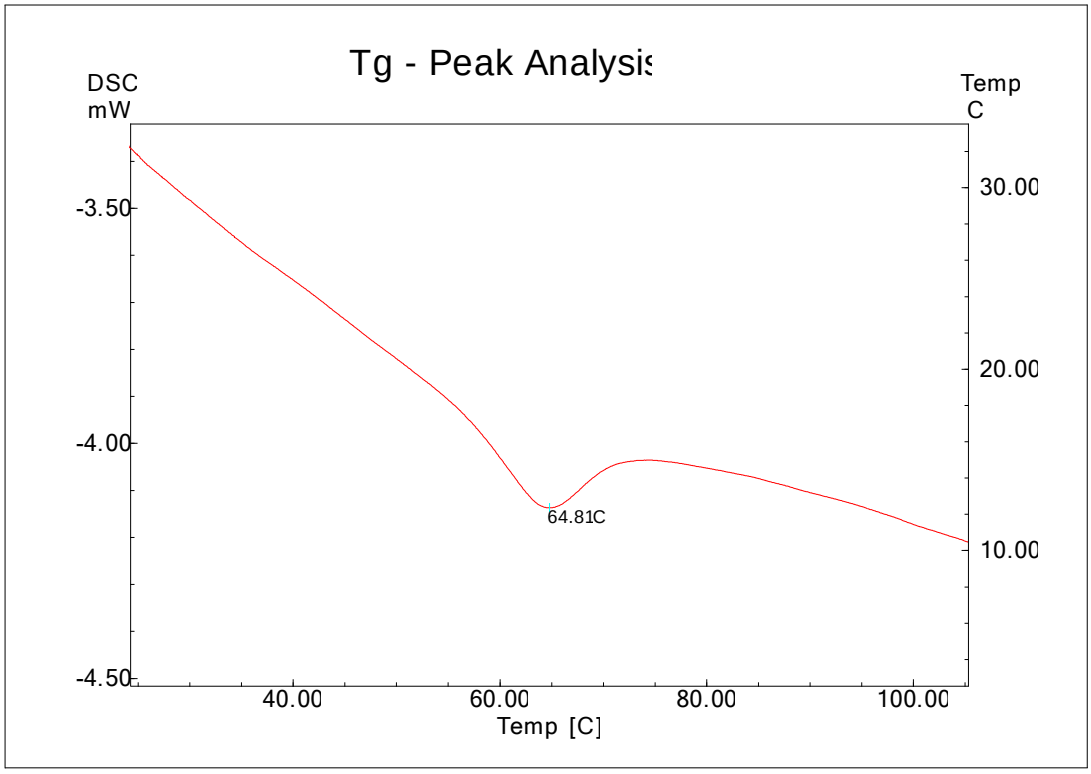

Figure 3.1: DSC T_g peak analysis of a dichloromethane-cast MEH-PPV film (under vacuum atmosphere)

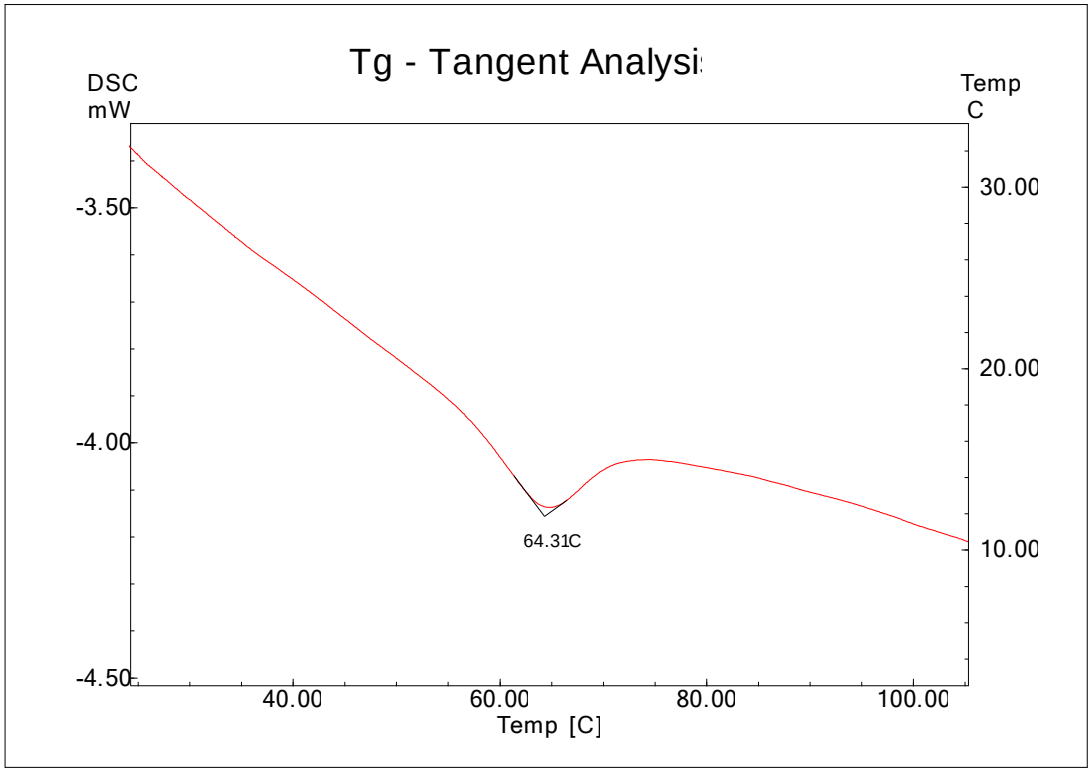

Figure 3.2: DSC T_g tangent analysis of a dichloromethane-cast MEH-PPV film (under vacuum atmosphere)

Triplicates of films of each different solvent-atmosphere condition were made and analyzed. The averages and standard deviations (Equation 1) of each triplicate T_g analyzed by peak analysis were calculated and summarized in Table 3.1. The averages and standard deviations of each triplicate T_g analyzed by tangent analysis were calculated and summarized in Table 3.2.

$$\sqrt{\frac{\sum (x-\bar{x})^2}{(n-1)}}$$

Equation 1. Standard deviation formula

	Argon	Air	Vacuum
CB-Cast	66.12, ±1.02	66.57, ±0.54	68.26, ±0.22
Tol-Cast	65.89, ±0.70	65.55, ±0.84	65.99, ±0.29
CF-Cast	64.41, ±0.26	65.57, ±0.52	66.14, ±0.41
DCM-Cast	63.91, ±1.44	65.52, ±0.28	65.20, ±0.54

Table 3.1: Average DSC T_g and standard deviation results in °C using peak of the transition curve

	Argon	Air	Vacuum
CB-Cast	64.29, ±0.21	64.99, ±0.10	67.03, ±0.22
Tol-Cast	64.24, ±0.70	64.66, ±0.95	64.78, ±0.42
CF-Cast	63.38, ±0.19	64.07, ±0.51	65.49, ±0.08
DCM-Cast	62.97, ±1.05	64.05, ±0.47	64.30, ±0.28

Table 3.2: Average DSC T_g and standard deviation results in °C using lines tangent to the transition curve

The average T_g values obtained using four different solvent cast films (and 3 different atmospheric conditions) were overlaid for both methods of determining the T_g: using peak of the transition curve and lines tangent to the transition curve in Figures 3.3 and 3.4, respectively. Chlorobenzene-cast films, having the highest average T_g, were graphically compared to each solvent-cast film individually, and the average standard deviation of all 3 atmospheres (vacuum, air, argon) used for each (see Appendix, Figures A-1 to A-6). This was done to evaluate significant statistical differences between the glass transition temperatures of films cast from different solvents, and under different atmospheric conditions.

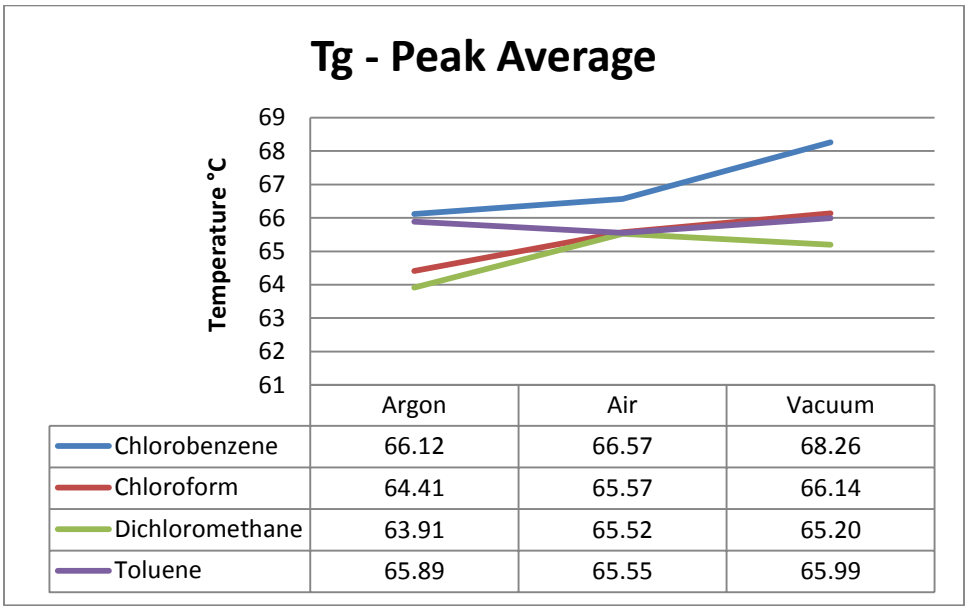

Figure 3.3: Overlay of the average DSC T_g values using peak of the transition curve

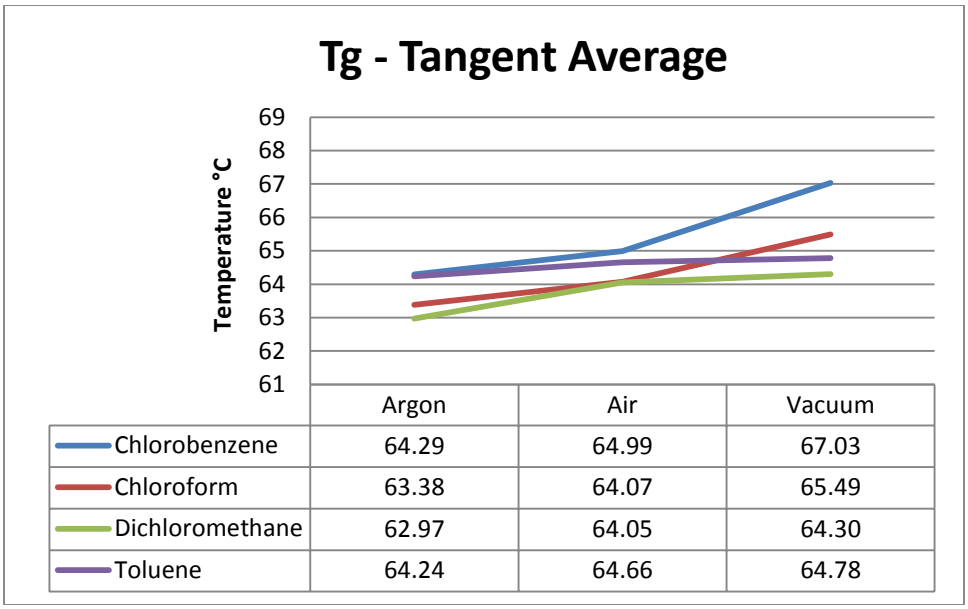

	Argon	Air	Vacuum
Chlorobenzene	64.29	64.99	67.03
Chloroform	63.38	64.07	65.49
Dichloromethane	62.97	64.05	64.30
Toluene	64.24	64.66	64.78

Figure 3.4: Overlay of the average DSC T_g values using lines tangent to the transition curve

MEH-PPV films cast from chlorobenzene exhibit a T_g that is higher than chloroform, dichloromethane, and toluene-cast films based on average measurements (Table 3.1 and Table 3.2). There is a significant difference in T_g between chlorobenzene, and both dichloromethane and chloroform-cast films cast under argon and vacuum using peak analysis, (see Appendix, Figures A-1 and A-2). A significant difference between chlorobenzene and toluene-cast films under vacuum was also observed (see Appendix, Figure A-3). Using lines tangent to the transition curve to calculate the T_g yielded significant differences between chlorobenzene and both dichloromethane and chloroform-cast films under argon, air and vacuum (see Appendix, Figures A-4 and A-5). Toluene and chlorobenzene-cast films under vacuum were the only significant differences (See Appendix, Figure A-6), same as with the peak analysis method.

Discussion

There is more variability when using the software automated peak analysis to find the glass transition, possibly because transition curves are not all uniform, which can have an effect on where the peak occurs. The variability would also indicate that this may not be the most reliable method (in comparison to the line tangent method). Overall, the glass transition

temperatures agreed with literature values of 60-70°C (since instrument and analysis method are rarely reported, a more accurate comparison is not available at this time).[22, 32-34]

There were differences between glass transition temperatures of chlorobenzene-cast films, and those cast from chloroform and dichloromethane, especially under vacuum. This should be expected: aromatic solvents preferentially solvate the aromatic backbone of the polymer; in an aromatic solvent, MEH-PPV will unfold to maximize favorable π-π interactions between the polymer and solvent, and the chains adopt a rigid, open conformation.[13, 14] With a more open conformation, the polymer will have a higher number of longer conjugation length segments.[13, 16, 27] With an increase in conjugation length, chain mobility decreases, and the strength and glass transition temperature of the polymer increases.

Casting under vacuum should yield films that are closer to their solution morphologies, as the solvent is removed more rapidly and the chains are not allowed as much time to relax to a lower energy state. Chlorobenzene-cast films differed significantly from every other solvent-cast film under vacuum.

C. Specific Heat Capacity

Specific heat capacity is the amount of heat energy required to increase the temperature of a sample by one degree (with respect to sample mass).

$$C = \frac{q}{m*T}$$

Equation 2. Specific heat capacity

There are many factors that can affect and alter the specific heat capacity of a polymer, including the degree of crystalline and amorphous regions, impurities or plasticizers in the sample, oxidation, etc. When used in devices which operate at higher than ambient temperatures, an increase in heat capacity could prove critical to device operability (i.e. charge through LED; photovoltaics). Polymers which are completely amorphous have specific heat

capacity values that are greater than crystalline/semi-crystalline polymers of the same make-up.[35] It would therefore be beneficial to (most) device operation to produce films with less crystalline domains.

There are several ways to determine the specific heat capacity, with differential scanning calorimetry being one of them. The experimental procedure for determining the specific heat capacity by DSC can be found in ASTM E1269, and this method was employed for this project.

A series of at least 3 DSC measurements must be taken in order to obtain the C_p (heat capacity under constant pressure; standard notation). Note that in all cases an empty pan is used on the reference side of the furnace. Sample measurements include:

1. Empty pan
2. Empty pan + unknown C_p material (sample under study)
3. Empty pan + known C_p material (reference – sapphire disk or α-alumina)

Once these measurements are taken, a calculation program in the software can compute the specific heat capacity of the sample of the temperature range of study. An example overlay of the 3 analyses can be seen in Figure 3.5:

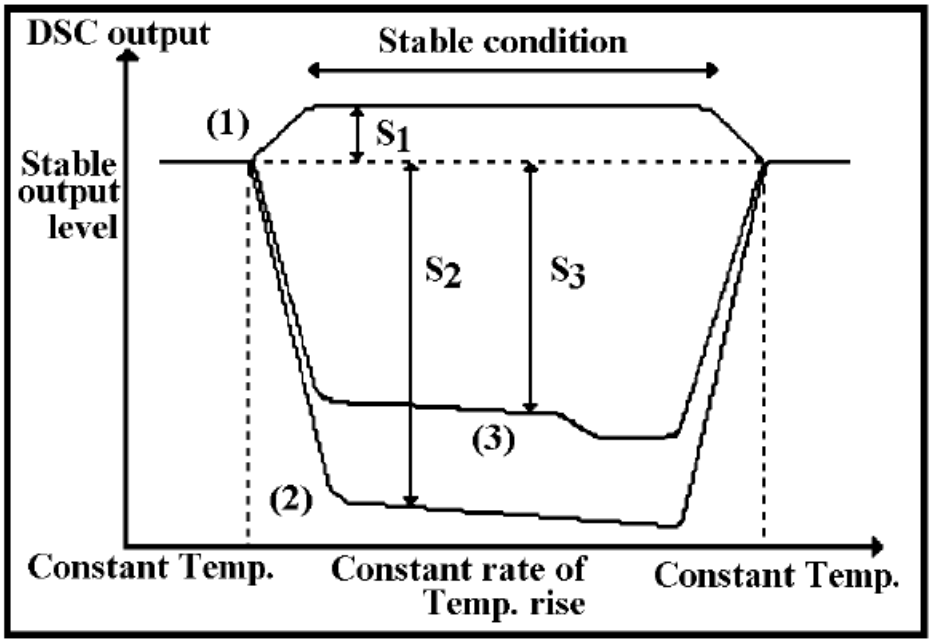

Figure 3.5: Overlay of specific heat measurements: (1) empty pan; (2) empty pan + sample under study; (3) empty pan + reference material. [36]

The following formulas correspond to the analysis of the sample measurements above respectively:

Equation 3. $KS_1 = C_s^h - C_r^h$

Equation 4. $KS_2 = \left(C_s^h + m_0 c_0\right) - C_r^h$

Equation 5. $KS_3 = \left(C_s^h + mc\right) - C_r^h$

K is a proportion constant, $S_{1\text{-}3}$ are DSC signals (Figure 3.5), $C_s^h \; and \; C_r^h$ are heat capacities for the sample and reference sides of the DSC furnace respectively, m is sample under study mass, m_0 is reference sample mass, and c_0 and c are reference sample under study samples respectively.

Combined, the above equations (Equations 3.5) produce an equation for the specific heat capacity of the sample under study:

Equation 6. $C = \frac{m_0 c_0}{m} x \frac{S_3 - S_1}{S_2 - S_1}$

Samples of each solvent-cast film, under atmospheric conditions of vacuum, argon, and air, were analyzed in triplicate. The results of each test were recorded into data table (Table 3.3). Once a triplicate was complete, the results were averaged together and their standard deviations calculated (Table 3.4).

Chlorobenzene - Argon		
°C	**°K**	**Cp (J/g·K)**
50.0	323.1	2.122
55.0	328.1	2.172
60.0	333.1	2.235
65.0	338.1	2.282
70.0	343.1	2.273
75.0	348.1	2.268
80.0	353.1	2.285
85.0	358.1	2.310
90.0	363.1	2.334
95.0	368.1	2.358
100.0	373.1	2.380
105.0	378.1	2.404
110.0	383.1	2.429
115.0	388.1	2.430

Table 3.3: Table of DSC C_p measurements for chlorobenzene-cast MEH-PPV films under argon atmosphere

CB - Ar - Avg.		
°C	**Cp (J/g·K)**	**StdDev.**
50.0	2.233	0.20
55.0	2.280	0.19
60.0	2.341	0.18
65.0	2.385	0.18
70.0	2.376	0.19
75.0	2.376	0.20
80.0	2.392	0.20
85.0	2.417	0.20
90.0	2.440	0.20
95.0	2.461	0.20
100.0	2.480	0.20
105.0	2.502	0.20
110.0	2.524	0.20
115.0	2.523	0.20
	StdDev. Avg.	0.20

Table 3.4: Table of average DSC C_p measurements with standard deviation for chlorobenzene-cast MEH-PPV films under argon atmosphere

Once all the specific heat capacity averages with standard deviation were calculated, the results were overlaid in order to compare films cast using different solvents (Figure 3.6) and under different atmospheric conditions (Figure 3.7). The films with the highest and lowest specific heat capacities were individually compared with standard deviation calculations to determine the significance, if any, of these differences (Figure 3.8).

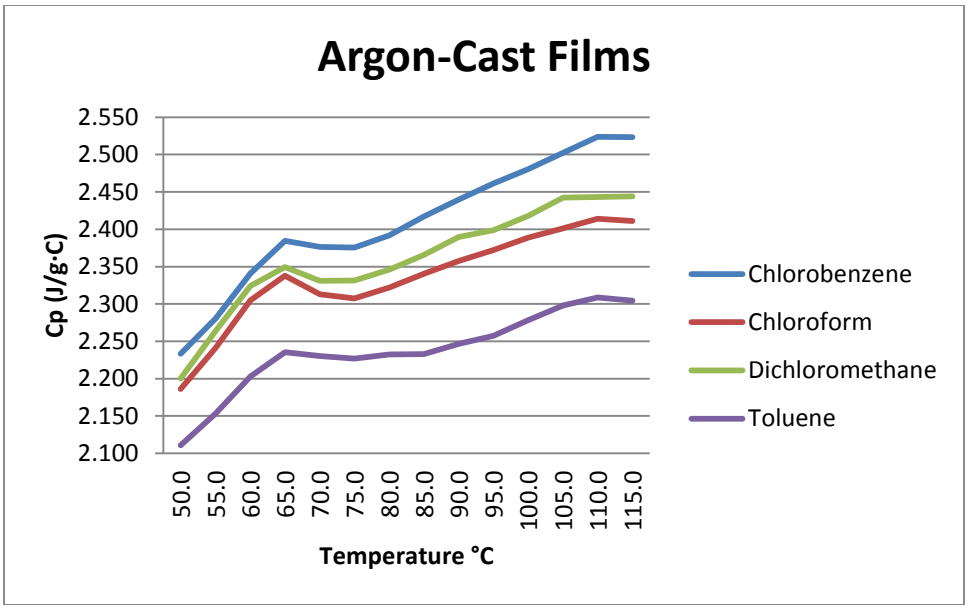

Figure 3.6: Overlay of average DSC C_p measurements for argon-cast films (using different solvents)

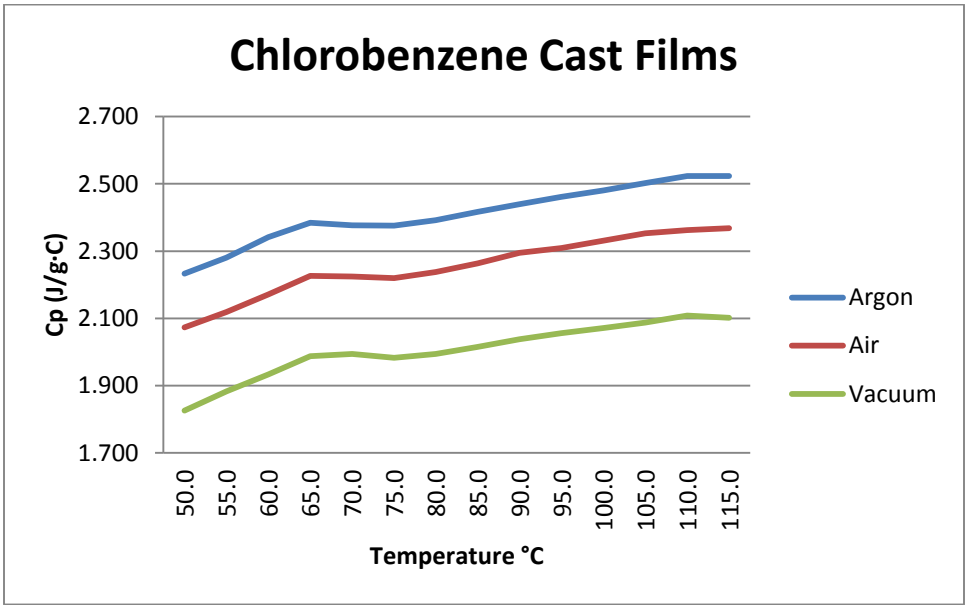

Figure 3.7: Overlay of average DSC C_p measurements for chlorobenzene-cast films (under different atmospheric conditions)

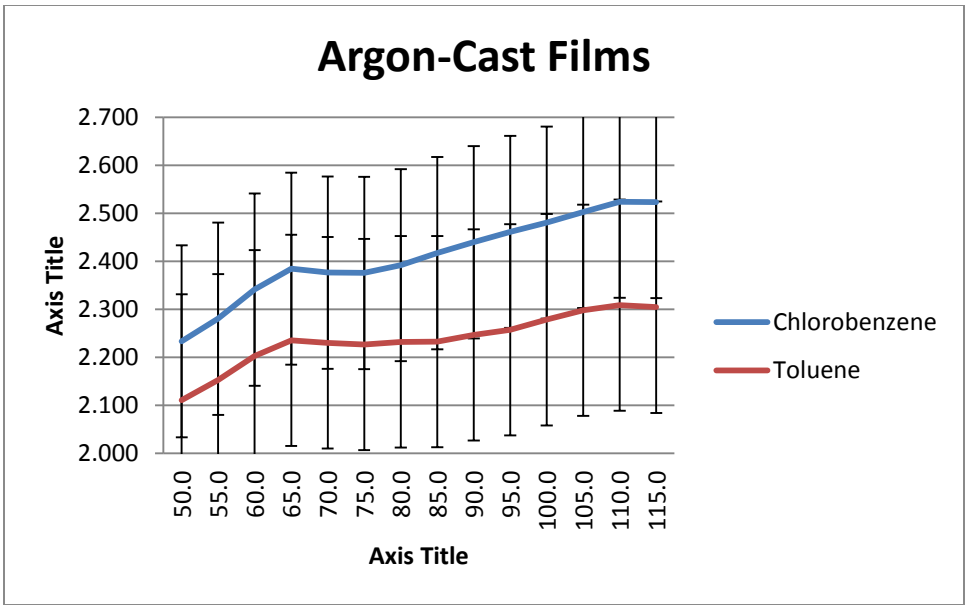

Figure 3.8: Overlay of average DSC C_p measurements for argon-cast films (using chlorobenzene and toluene) with standard deviations

MEH-PPV films cast from chlorobenzene had a significantly higher average C_p than chloroform-cast films under air atmosphere (see Appendix, Figure A-8). While under a vacuum atmosphere, films cast from chloroform and dichloromethane had higher C_p's than films cast from toluene and chlorobenzene, although not significantly (see Appendix, Figure A-9). Films cast in each solvent showed the same trend in C_p measurements, with C_p under Argon greater than that of air and vacuum (Figure 3.8; see Appendix, Figures A-12, 14, 16). The only significant differences within films cast from the same solvent were in chloroform (see Appendix, Figure A-13) and toluene-cast (see Appendix, Figure A-17) films.

Discussion

We would expect that under a vacuum atmosphere, the specific heat capacities of chloroform and dichloromethane-cast films would be similar, and different than films cast from chlorobenzene and toluene. It has been reported that films cast from chloroform exhibit lower crystallinity than films cast from toluene.[35] Since crystalline domains lower the specific heat capacity of polymers, it would be expected that the chloroform and dichloromethane-cast

films would have higher specific heat capacity measurements than the aromatic toluene and chlorobenzene.

In solution, aromatic and aliphatic solvents have different interactions with the polymer, creating different chain morphologies. These differences have been known to carry over into the films when they are cast rapidly and the chains do not have time to relax into a lower energy state. Vacuum atmosphere is the most rapid processing method used in this study, and therefore it is expected that differences would be more pronounced under these conditions.

II. Differential Mechanical Analyzer (DMA)

A. Introduction

A differential mechanical analyzer (DMA) applies an oscillatory (sinusoidal) stress on a sample and measures the corresponding displacement (strain). This strain will show both the elastic and viscous response of the material.

A material that displays 100% viscosity or flow is referred to as Newtonian. This type of material deforms at a constant rate when a stress is applied, and the deformation is irreversible. For a material to follow Hookean Law (purely elastic), it will undergo instantaneous deformation, yet return to its original shape when the stress is removed: there is no loss of energy (i.e. spring).

Most materials are neither purely viscous nor purely elastic: they fall somewhere in between, in what is referred to as the viscoelastic region. If a material was purely elastic, the strain signal during DMA analysis would follow the stress, and a phase angle (δ) = 0° would be observed (in-phase). For a purely viscous material, the phase shift would be = 90° (out-of-phase). Any material in the viscoelastic region would therefore have a phase angle that falls $0 < \delta < 90°$.

From the phase angle δ, the storage modulus (E') and loss modulus (E") can be calculated. The storage modulus measures the stored energy in a sample, the elastic portion, while the loss modulus measures energy dissipated as heat (viscous portion). The ratio of these two moduli gives the tan δ.

Similar to the differential scanning calorimeter (DSC), DMA can also give the glass transition temperature (T_g) of a polymer. Whereas DSC measures heat flow and heat capacity, DMA measures mechanical strength and energy loss. At the glass transition, there is a dramatic decrease in the storage modulus (E'), and the loss modulus (E") reaches a maximum, making DMA more sensitive than the DSC.

The glass transition temperature using DMA can be evaluated several ways: the onset of a storage modulus drop, peak in the loss modulus, and peak temperature of tan δ can all be used as reported values for the T_g. The first historical value of the DMA T_g was reported as the peak temperature of the tan δ curve. This peak describes the damping characteristics of a material, and is usually higher than reported values using the peak of the loss modulus. The T_g value from the peak temperature of the tan δ curve > peak value of the loss modulus > onset of drop in storage modulus. As the peak temperature of the loss modulus is reached, the material undergoes a maximum change in polymer mobility, which itself is the definition of T_g. Many factors can affect the value of the T_g, including oscillation frequency, temperature ramp, atmospheric condition (temperature/humidity), and time. An oscillation frequency of 1Hz is generally accepted as the standard to give comparable T_g values to other thermal techniques. As with the DSC, DMA tests to evaluate the T_g should be started at least 50°C below the estimated value. This is especially important in order to observe the full change in the storage and loss modulus.

Changing the solvent and casting conditions by which MEH-PPV films are prepared has resulted in different morphologies and degrees of aggregation/conjugation length.[12, 13, 16-21, 23, 24, 26-31] It has been shown with nano-indentation experiments that chloroform (non-aromatic)-cast films yield higher and stronger mechanical properties such as hardness, Young's modulus and critical bending radius than toluene (aromatic)-cast films, due to the tight coil conformation of the polymer chains (stronger atomic and molecular bonding).[15] X-ray diffraction (XRD) scans have shown that this can affect crystalline domains and structure. [21] These altered morphologies and crystalline structure should be observable with DMA analysis through changes in the storage and loss modulus, as well as shifts in the glass transition temperatures. Since electroluminescent polymer films like MEH-PPV are used in devices which run current (LED) or operate under extreme conditions (Solar Cell), it is important to understand how these properties are affected by casting conditions.

B. Experimental Method

MEH-PPV film samples of ~13mm x 7.00mm x 0.020mm were cut with a fine razor blade and measured with calipers. Samples were placed into a film tension clamp. A torque wrench was used to secure the samples with an applied force of 0.2-0.3lbf. Samples were run in ambient conditions with no external purge gas introduced into the system under the following conditions:

1. Amplitude 15
2. Single Frequency = 1Hz
3. Isothermal Hold @ 35°C for 2 minutes
4. Ramp 1°C/min to 120°C

Films were run on a TA Instruments DMA 2980 with TA Software Version 1.1A. Test files were analyzed using TA Instrument's Universal Analysis software Version 4.2E. The T_g value for each test was evaluated as the peak height of the tan δ curve using the software's peak analysis

function (Figure 3.9). This value was chosen as the tests were not able to be run at 50°C or more below the T_g (lack of external cooling device); as a result, the storage and loss modulus curves were incomplete, and only the tan δ curve provided sufficient data.

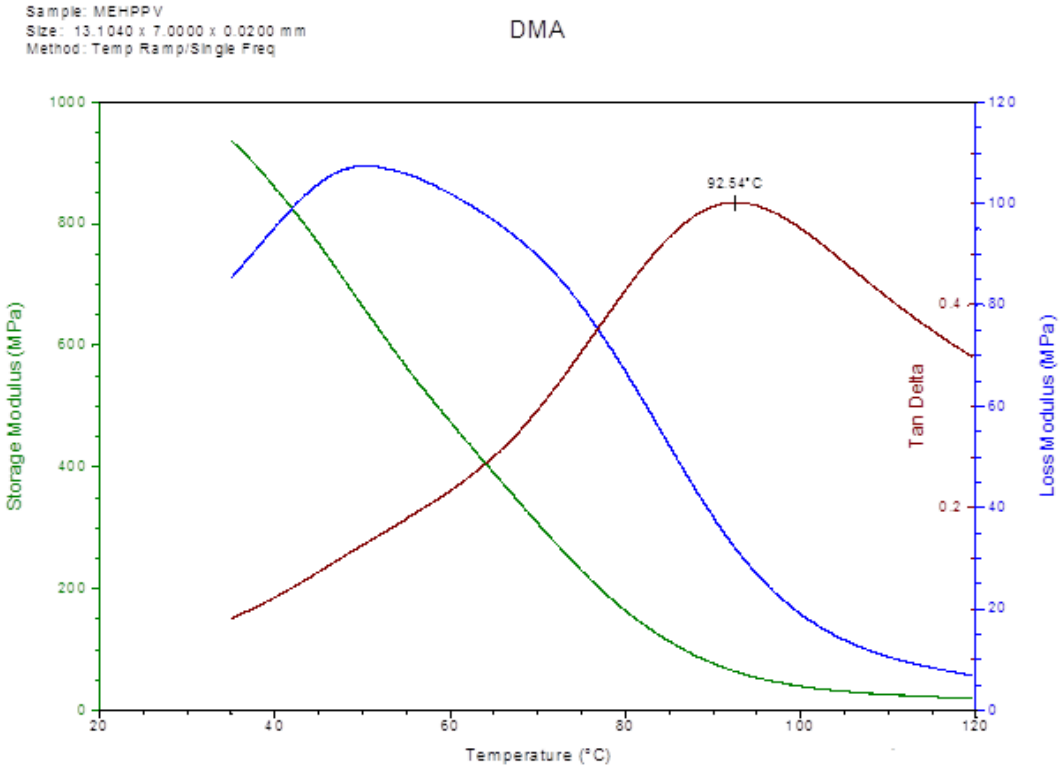

Figure 3.9: DMA peak analysis of MEH-PPV film for tan δ value

C. Experimental Results

MEH-PPV films cast from chlorobenzene, chloroform, toluene, and dichloromethane, and under vacuum, air and argon atmospheres were analyzed in triplicate on the DMA. The T_g measurements corresponding to the peak height of the tan δ analysis lines were averaged for each triplicate and summarized in Table 3.5 with standard deviation.

	Argon	Air	Vacuum
CB-Cast	84.77, ±4.57	91.89, ±3.46	92.68, ±4.48
Tol-Cast	72.40, ±4.97	77.94, ±4.54	85.34, ±1.55
CF-Cast	82.78, ±4.98	92.21, ±4.28	86.12, ±4.55
DCM-Cast	73.54, ±3.64	79.12, ±8.40	68.34, ±3.93

Table 3.5: Average DMA T_g and standard deviation results in °C using temperature corresponding to the peak height of the tan δ analysis lines

The average T_g's for each MEH-PPV casting condition were overlaid (Figure 3.10). Chlorobenzene-cast films, having the highest average T_g (chloroform cast films under air were slightly larger by 0.32°C), were graphically compared to each solvent-cast film individually, and the average standard deviations incorporated (see Appendix, Figures A-18 to A-20). This was done to look at significant statistical difference between the glass transition temperatures of films cast from different solvents, and under different atmospheric conditions.

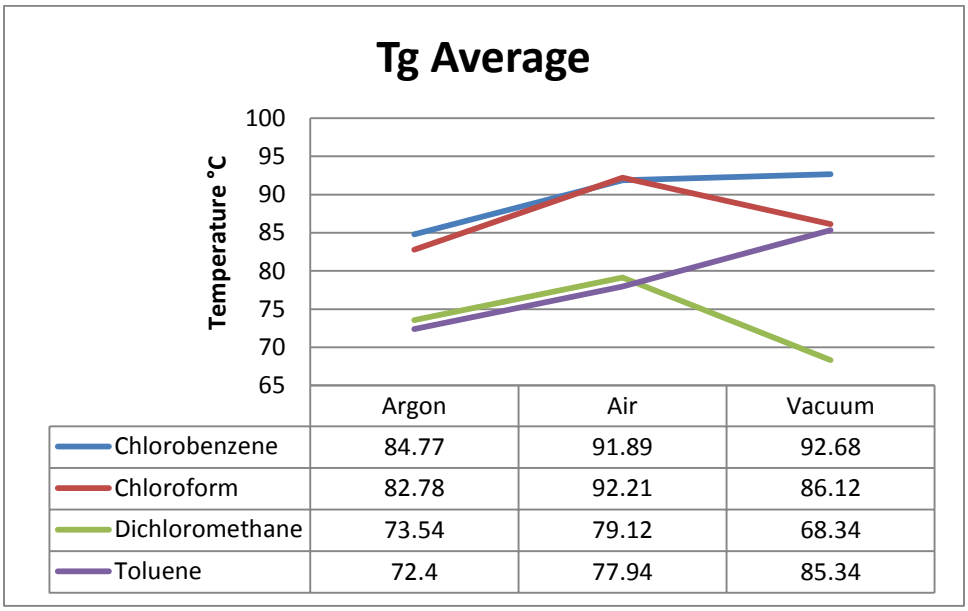

Figure 3.10: Overlay of the average DMA T_g measurements using temperature corresponding to the peak height of the tan δ analysis lines

D. Discussion

MEH-PPV films cast from chlorobenzene have a significantly higher glass transition temperature than films cast from toluene and dichloromethane for each casting atmosphere (see Appendix, Figures A-18 to A-20). These results coincide similarly with T_g

analysis performed using DSC, where CB-cast films had higher T_g's than chloroform and dichloromethane.

Literature values for the glass transition (T_g) temperatures of polymer films can vary greatly depending on the casting conditions, experimental conditions, and analysis parameters. Analysis of spin-coated, chloroform-cast films of MEH-PPV (2K/min heating rate, frequency sweep, 10mm long, ~5mm wide, ~0.02mm thick) showed two broad relaxation processes for both the storage and loss modulus: at 340 and at 220 K (previously assigned to α- and β-relaxation processes respectively).[34] This α-relaxation process at 340 K is consistent with other literature values of T_g determined using DSC.[34] In general, the T_g value from the peak temperature of the tan δ curve > peak value of the loss modulus > onset of drop in storage modulus. The T_g values obtained in this experiment using the DMA were determined from the peak of the tan δ curve, as this is the more common value represented: however, to date there have been no known values in the literature using this analysis point for MEH-PPV films.

There can be as much as a 20-25°C temperature difference in the range of values recorded for the T_g,, depending on the instrument (DSC, DMA, TMA) and analysis method (point on the DSC curve, storage modulus, loss modulus, tan δ peak). The T_g values of this study range from ~68 - 93°C using the peak of the tan δ curve.

The instrument used for these experiments had many mechanical errors during the time frame that the samples were run. Each mechanical error required a reboot and complete re-calibration of the system. The films were also analyzed over the course of several months. During this time the temperature and humidity inside the test lab fluctuated greatly. Material and polymer properties (such as storage and loss modulus) can be greatly affected by changes in atmospheric testing conditions. Since the T_g was calculated based on the tan δ, which itself is a function of both the storage and loss modulus, the combination of changing lab

conditions and mechanical errors leave doubts about the accuracy of the DMA data. Not being able to start the testing at 50°C or more below the T_g provided insufficient storage and loss modulus data, which would have been useful to provide insight into changes in chain conformation and film morphology under the various casting conditions. Further testing will need to be performed on a different instrument under more controlled testing conditions.

III. Thermogravimetric Analyzer (TGA)

A. Introduction

A thermogravimetric analyzer (TGA) is a thermal analysis technique which measures the mass change of a sample as it is heated. These mass changes are displayed on a thermogram, which graphically displays the increasing or decreasing change in mass as a function of time or temperature. Oxidation, decomposition, and loss of volatiles are common uses of a TGA.

The TGA consists of a small sample (2-20 mg) residing within a sample pan, usually platinum (quartz, alumina and aluminum are alternatives depending on temperature range). The sample pan is suspended from a balance mechanism by a suspension wire, typically with a small stage for support. A furnace is raised over the sample, fully encapsulating it. The furnace has o-rings to seal the connection with the rest of the instrument, and allow the user to control the atmosphere inside. The sample can be purged with nitrogen or argon gas, or introduced to a steady flow of air (compressed air) to encourage or hinder reactions. Reactive gases may also be introduced, as can water vapor.

The TGA has been used as a tool for measuring the thermal stability of polymer films and their blends.[22, 37-39] Many factors can play a role in determining thermal stability, such as bond energies, plasticizers/fillers, steric factors, oxidative effects, and internal mechanical stresses to name a few. There have been reported differences in decomposition rates between MEH-PPV films of different molecular weights, as well as the atmosphere under which the

samples were analyzed.[22, 38] MEH-PPV films with a molecular weight of 51 and 86 kg·mol^{-1} have been shown to undergo a two-step decomposition (under purged inert atmosphere), whereas films with a molecular weight of 125 kg·mol^{-1} underwent a single step degradation.[22] In another study, it was shown that analyzing MEH-PPV under nitrogen resulted in a two-step decomposition, where air yielded a multi-step.[38]

The thermal stability and degradation rates of MEH-PPV are important in the fabrication of devices, as greater stability will increase the application potential. MEH-PPV films that are cast under different conditions result in different morphologies, which could potentially alter the thermal stability of the films, resulting in varying degradation rates and onset temperatures.

B. Experimental Method

MEH-PPV film samples were cut into strips of ~2.0 mg (±0.1 mg). The samples were placed inside aluminum pans and loaded onto the TGA. Samples were equilibrated at 50°C and run under a nitrogen purge gas introduced into the system. Heating rates of 1, 10 and 20°C/min were used for comparison, with final temperature of 550°C.

Films were run on a TA Instruments TGA 2050 with TA Software Version 1.1A. Test files were analyzed using TA Instrument's Universal Analysis software Version 4.2E.

C. Experimental Results

MEH-PPV films cast from chlorobenzene and chloroform, and under vacuum, air and argon atmospheres were analyzed on the TGA at heating rates of 1, 10 and 20°C/min. The decomposition weight loss thermograms were overlaid to give comparisons on the thermal stability.

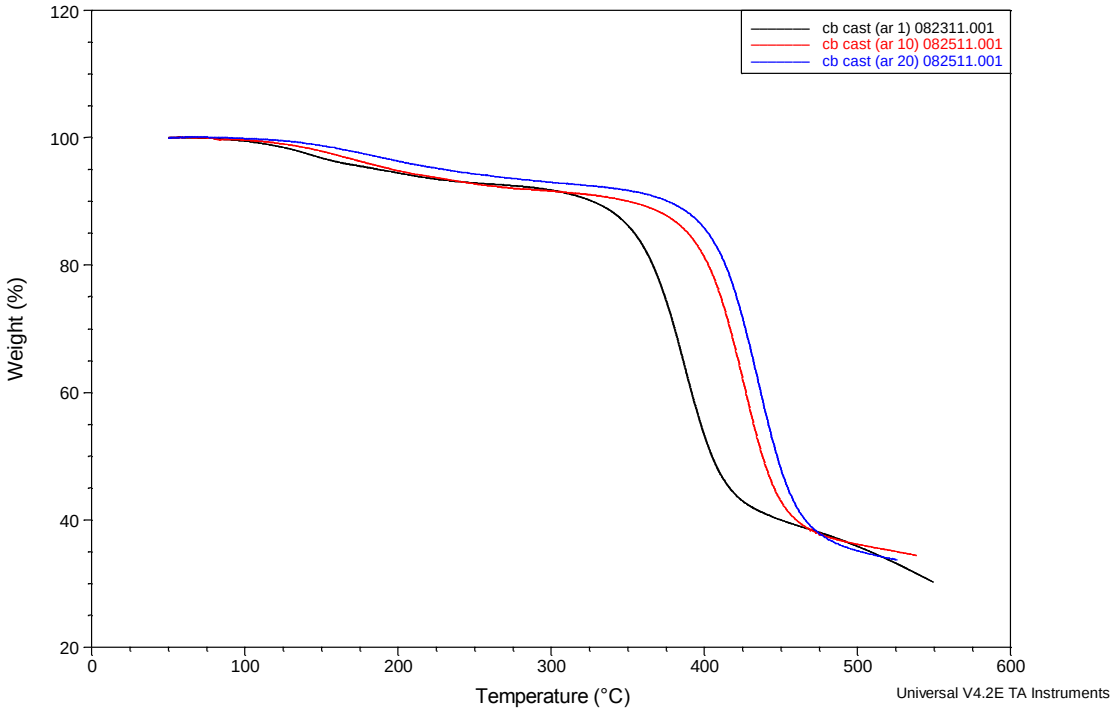

Figure 3.11: Overlay of chlorobenzene- cast MEH-PPV films (under argon), heated at 1, 10 and 20°C/min using TGA

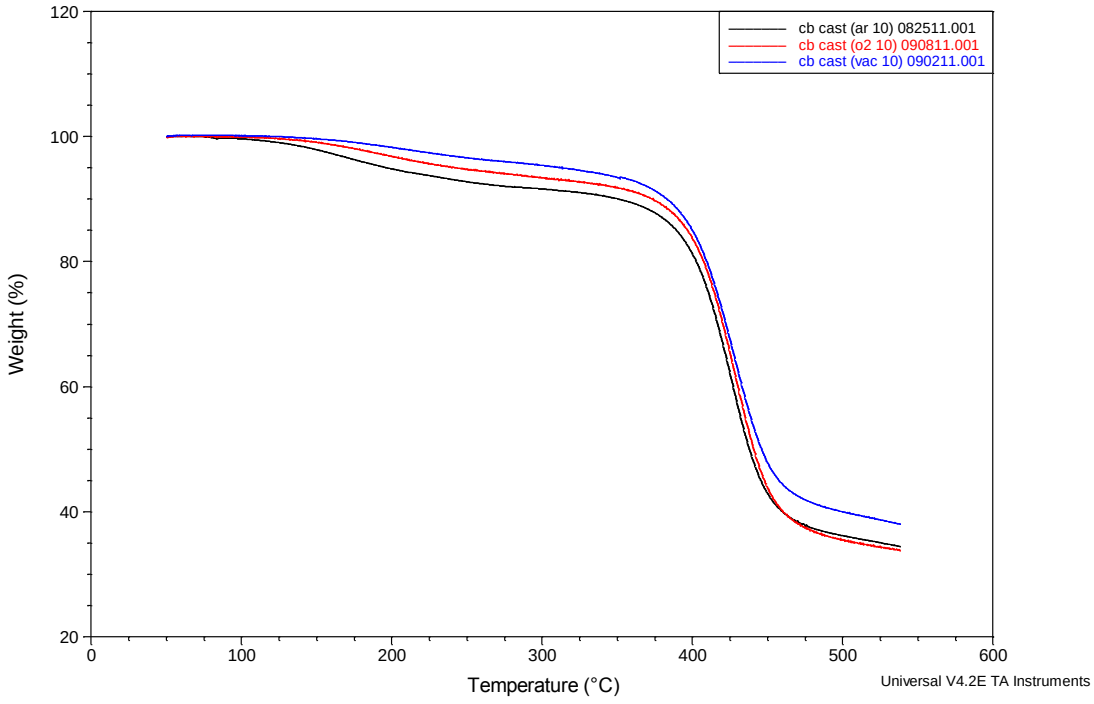

Figure 3.12: Overlay of chlorobenzene- cast MEH-PPV films (under argon, air and vacuum), heated at 10°C/min using TGA

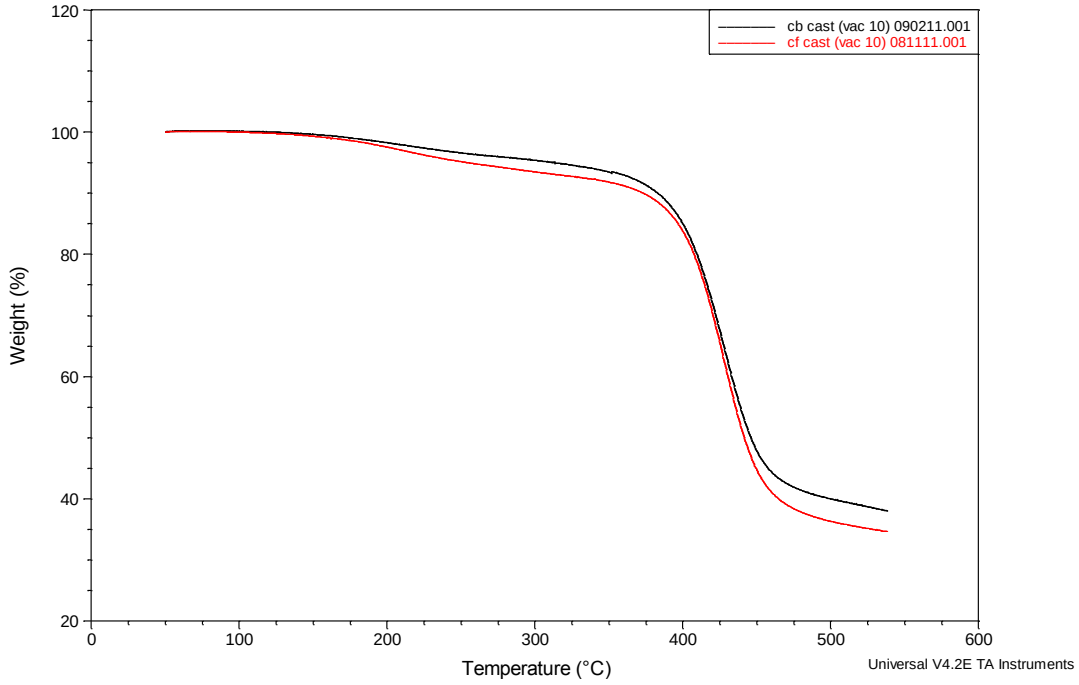

Figure 3.13: Overlay of chlorobenzene and chloroform- cast MEH-PPV films (under vacuum), heated at 10°C/min using TGA

As the heating rate of the TGA increases, the decomposition curves of the MEH-PPV films shift to the right (higher temperature) of the thermogram. With a constant heating rate, the MEH-PPV films cast under argon appear to have the earliest onset degradation temperature, as well as the most pronounced two-step loss. This is followed by films cast under air (in the fume hood), and those cast under vacuum have the most thermal stability.

Under the same atmosphere, chloroform-cast films appear to degrade faster than the chlorobenzene-cast films. However, with only 1 or 2 samples from each batch tested under the different conditions, no statistical calculations can be performed.

D. Discussion

Preliminary work on analyzing MEH-PPV films cast under different conditions has been done to gain familiarity with the technique, as well as provide initial data for comparison. In this study, MEH-PPV films with an average molecular weight of M_n=70,000-

100,000 were analyzed using TGA under a steady stream of nitrogen. It has been previously reported that nitrogen purge, as well as molecular weights of 51 and 86 $kg \cdot mol^{-1}$ produce thermograms with a two-step weight loss profile.[22, 37, 38] The results in this study confirmed these previous observations.

There were differences in the degradation profile of films cast from different solvents, as well as those cast under different atmospheres (constant heating rate). This compares well with other analytical techniques performed in this study. A larger sample set will need to be analyzed going forward in order to perform statistical calculations on the results, as well as develop a better understanding of the mechanism and theory behind these observations.

The focus of this preliminary work focused solely on the weight loss profiles of the films. Future work will expand on this as well as on the activation energies of these step losses, and the lifetime prediction calculations of the polymer film at different temperatures.[37, 38]

IV. Thermal Analysis Summary

Electroluminescent polymer films like MEH-PPV are used in many devices, some of which apply current (LED)/(LET),[4, 9, 10, 40] or operate under extreme conditions (Photovoltaics).[41] As a result, it is important to understand how properties such as the glass transition temperature (T_g) and specific heat capacity (C_p) are affected by processing conditions. It was the intent of this study to use the thermal analysis techniques of differential scanning calorimetry (DSC), differential mechanical analysis (DMA), and thermogravimetric analysis (TGA) to evaluate thermal properties, including the glass transition temperature and specific heat capacity of MEH-PPV films.

It has been well documented that changing the solvent and casting conditions by which MEH-PPV films are prepared result in different morphologies and degrees of aggregation/chain length.[12, 13, 16-21, 23, 24, 26-31] The processing conditions of the MEH-PPV films in this study were changed by casting in 4 different solvents, including the aromatic solvents chlorobenzene and toluene, and the aliphatic solvents chloroform and dichloromethane. Aromatic solvents preferentially solvate the aromatic backbone of the polymer; in an aromatic solvent, MEH-PPV will unfold to maximize favorable π-π interactions between the polymer and solvent, and the chains adopt a rigid, open conformation.[13, 14] With a more open conformation, the polymer will have a higher number of longer conjugation length segments.[13, 16, 27] With an increase in conjugation length, chain mobility decreases, and the mechanical strength and glass transition temperature of the polymer increases.

Each MEH-PPV film cast under a different solvent was also cast under three different atmospheric conditions: vacuum, argon and air. These were the ranges available from slow-solvent evaporation (argon), to a more rapid evaporation of the solvent (vacuum). Rapid evaporation of highly volatile solvents yields films which retain many of the characteristics of the solution.[13] For the tight coils formed in polymer-aliphatic solvent solutions, there is too little time for them to adopt a more open conformation before the solvent has evaporated.[13]

The aromatic solvents chlorobenzene and toluene should yield the highest T_g values when cast under vacuum atmosphere, since their favorable π-π interactions and high number of longer conjugation lengths should be preserved with the more rapid evaporation of the solvent. MEH-PPV films cast from chlorobenzene under vacuum had T_g temperatures that were significantly higher than values of other solvent-cast films. The same results were obtained using DMA, although the difference between the chlorobenzene and chloroform-cast film were not statistically significant.

Preliminary results on the TGA indicate that chlorobenzene-cast films have more thermal stability, and a slower degradation rate than chloroform-cast films (both cast under vacuum). Thermal stability also appears to be greatest in films cast under vacuum, followed by those under air (fume hood), with films cast under argon the least stable.

The DSC T_g values agreed with the glass transition temperatures reported in the literature (60-70°C).[22, 32-34] As with the DSC, DMA tests to evaluate the T_g should be started at least 50°C below the estimated value. This is especially important in order to observe the full change in the storage and loss modulus. For the DMA in this study, films were not able to be run at 50°C or more below the T_g (lack of external cooling device); as a result, the storage and loss modulus curves were incomplete, and only the peak tan δ curve provided sufficient data for T_g analysis. This peak describes the damping characteristics of a material, and is usually higher than reported values using the peak of the loss modulus. Therefore the results could only be qualitatively compared to those of DSC analysis. In general, DMA analysis of the T_g is frequency dependent, whereas DSC is heating rate dependent: therefore there will always be differences between the two values (as much as 20°C).

The glass transition temperature is dependent on many factors: one being the degree of crystallinity within the polymer. Increasing the degree of crystallinity raises the T_g of the polymer. This same increase in crystallinity has the opposite effect on the specific heat capacity (lowers it).

It has been reported that films cast from chloroform exhibit lower crystallinity than films cast from toluene.[35] Since crystalline domains lower the specific heat capacity of polymers, it would be expected that the chloroform and dichloromethane-cast films would have higher specific heat capacity measurements than those cast from aromatic toluene or chlorobenzene. In this study, films cast from chloroform and dichloromethane while under vacuum had higher

C_p's than films cast from toluene and chlorobenzene, although not significantly. In solution, aromatic and aliphatic solvents have different interactions with the polymer, creating different chain morphologies. These differences have been known to carry over into the films when they are cast rapidly and the chains do not have time to relax into a lower energy state. Vacuum atmosphere is the most rapid processing method used in this study, and therefore it is expected that differences would be more pronounced under these conditions.

Chapter 4: Spectroscopic Analysis

I. Fourier-Transform Infrared Spectroscopy (FT-IR)

A. Introduction

Infrared radiation (IR) is defined as the portion of the electromagnetic spectrum from ~10,000 – 100cm^{-1}. Organic molecules can absorb this radiation, resulting in molecular vibrations and rotations. In IR spectroscopy, if the energy changes associated with these molecular movements (vibrations, rotations) result in a net change in dipole moment, then the wavenumbers that correspond with each individual movement (vibration, rotation, wag, etc.) will appear as bands in the IR spectra.[42]

In the study of organic molecules using IR spectroscopy, two of the most important wavelength regions are the functional group region (4000-1300cm^{-1}), and the fingerprint region (1300-650cm^{-1}). In the functional group region, strong absorption bands result from stretching of hydroxyl, amine, carbonyl and CH_x groups. The fingerprint region is comprised of complex absorption patterns; however, in reference to other regions can be extremely valuable to interpretation and identification of a substance.

MEH-PPV films were compared with the literature to ensure that good quality samples had been produced: this includes comparing the IR spectra of the films with the IR spectra of the individual solvents (chlorobenzene, chloroform, toluene and dichloromethane), to ensure there are no residual solvents remaining in the films. There have been reported differences in the intensities of some of the absorption peaks of the MEH-PPV films cast from different solvents by reflection absorption mode FT-IR measurements.[29] There have been noticeable intensity changes in the C-H region (3100-2800cm^{-1}), with absorption peaks at 2958, 2930, 2872 and 2857cm^{-1}, as well as in the fingerprint region (1300-650cm^{-1}) with absorption peaks at 1208, 1042, 969, and 859cm^{-1} (Figure 4-1). It is theorized that the different solvents

yield distinct conformations and different aggregation styles of the polymer chains (in solution), yielding different surface energies.[29] As described previously (Figure 1.2), aromatic solvents tend to solvate the aromatic backbone of the polymer (parallel to the surface), whereas the nonaromatic solvents can be thought of as interacting, "perpendicular," to the surface (Figure 4-2). *In the reflection absorption mode FT-IR measurement, a vertically polarized source beam is used. Thus, the absorption from a vibration mode of the sample is expected to reach maximum when its transition dipole is normal to the sample surface, and reach minimum when the transition dipole is parallel to the sample surface.*[29] This would account for the intensity differences described in the literature based on the solvents used.

Oxidation, another factor to consider when casting polymer films, can be identified by absorption in the region from 1200-1100cm^{-1}. During device fabrication and operation, oxidation can play a key role in early degradation of the polymer film.[43] While oxidation is an inevitable process, any casting solvent or atmospheric condition that accelerates the process should be noted.

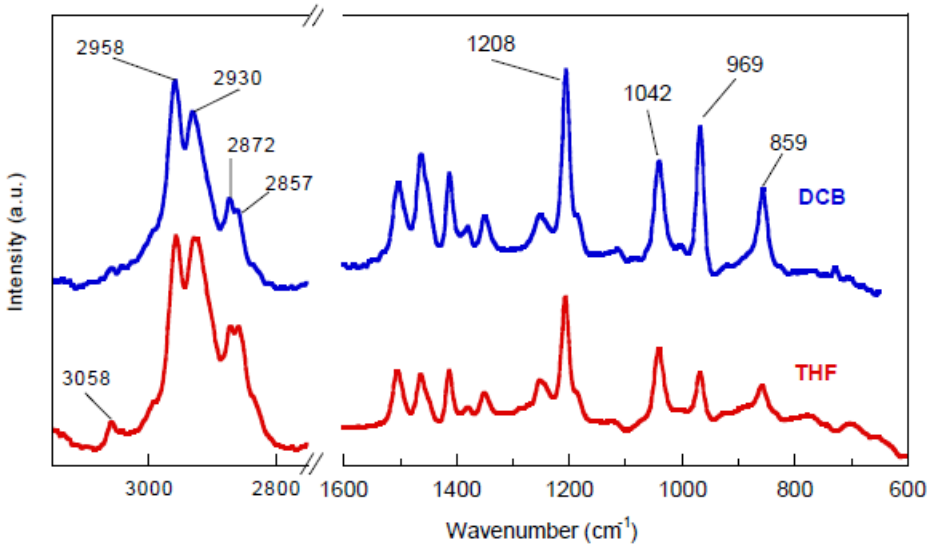

Figure 4.1: Reflection absorption FT-IR spectra of MEH-PPV films spun from dichlorobenzene (DCB) and tetrahydrofuran (THF) by Yang group.[29]

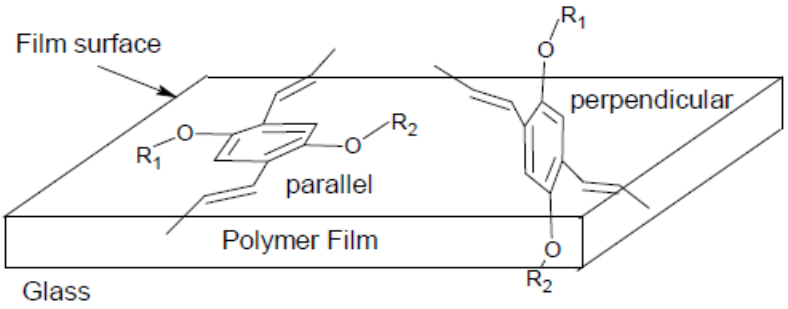

Figure 4.2: Two possible orientations of the aromatic ring on the substrate surface of MEH-PPV films (based on solvent) as drawn by Yang group.[29]

The C-H and fingerprint regions, as well as bands at 1600-1300cm^{-1} (skeletal bands for aromatics and heteroaromatics) of MEH-PPV films cast from different solvents, under different atmospheric conditions, were compared for morphological effects resulting in changes in intensity, band-width, and shifts in the absorption peaks. A table of expected values based on literature is summarized in Table 4-1.

Frequency (cm^{-1})	Assignment
3055	Vinyl stretching -CH
2960-2870	Asymmetric C-H stretching in $-CH_2$ & $-CH_3$ groups
1691	C=C stretching
1608	Asymmetric phenyl semi-circular stretch
1506	Semicircular phenyl stretch
1465	Asymmetric C-H bending in $-CH_2$ group
1415	Semicircular phenyl stretch
1380	Symmetric alkyl CH_2
1255	Aryl-alkyl ether (C-O-C) asymmetric stretching
1208	Phenyl-oxygen stretch; C-H deformation
1100-1200	Oxidation
1044	Aryl-alkyl ether (C-O-C) symmetric stretching
969	Vinylene CH wag
857	Out-of-plane phenyl CH wag

Table 4.1: Expected frequencies for IR spectra of MEH-PPV films based on literature.[44-46]

B. Experimental Method

MEH-PPV films were analyzed on a Bio-rad FTS 6000 spectrophotometer immediately after solvent evaporation was complete. Each film was cut into 5 pieces and run in triplicate (piece from middle and two sides used to obtain good sampling of the film). The results were analyzed using Varian Resolutions Pro Software Version 4.1.0.101.

Speed: 5KHZ
Filter: 1.2
UDR: 2
Resolution (cm^{-1}): 4
Sensitivty: 1
Scans to Co-add: 16
Background Scans: 16
Apodization Type: Triangle
Absorbance

C. Experimental Results

The peaks of each MEH-PPV film were calculated using the software and agree well with literature values (Figure 4-3). A representative spectrum was also compared to a spectrum of MEH-PPV powder prepared via K-Br pellet and analyzed (Figure 4-4): there seems to be no significant differences between the two.

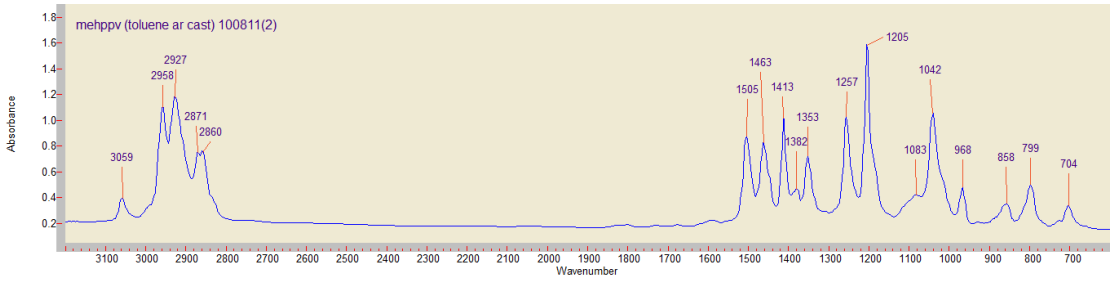

Figure 4.3: MEH-PPV Film (toluene cast in argon atmosphere) with peaks labeled

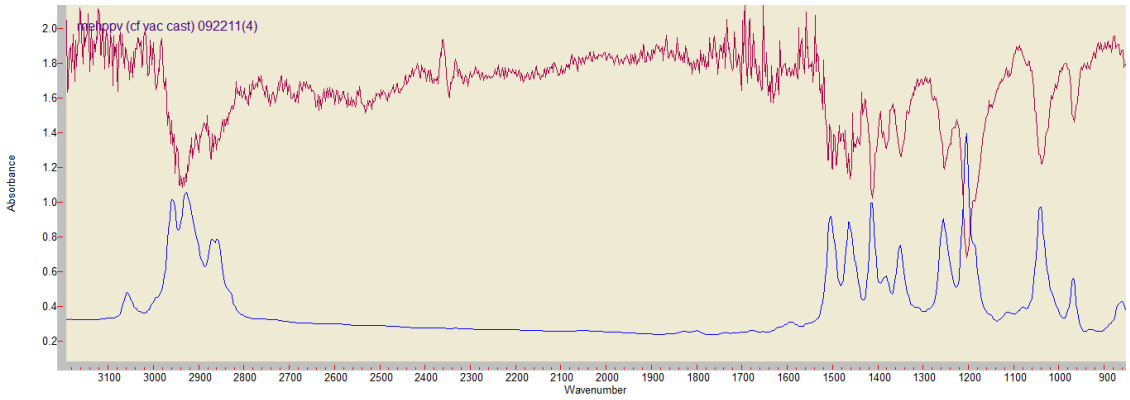

Figure 4.4: IR spectra overlay of MEH-PPV film cast from chloroform (under vacuum atmosphere) and MEH-PPV powder in K-Br pellet. The MEH-PPV in K-Br is displayed in transmittance (chloroform-cast film in absorbance) to better show corresponding peaks.

IR spectra of MEH-PPV films cast from each solvent and under different atmospheric conditions were overlaid. Since each film was analyzed in triplicate, a total of 9 individual spectra were overlaid for each casting condition. The spectra were truncated so that only the bands of interest (3100-2800cm^{-1} and 1600-650cm^{-1}) are visible (Figures 4-5 and 4-6, respectively). It should be noted that some IR spectra were only run to 800cm^{-1}, and bands between 800-650cm^{-1} are not available for analysis. Additional spectra can be found in the Appendix.

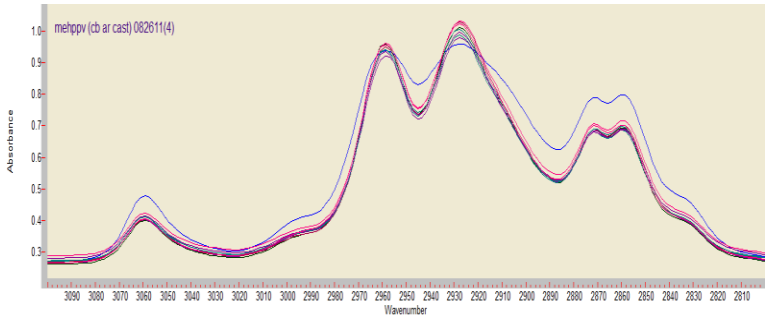

Figure 4.5: Overlay of MEH-PPV films cast from chlorobenzene under argon (3100-2800cm^{-1} region)

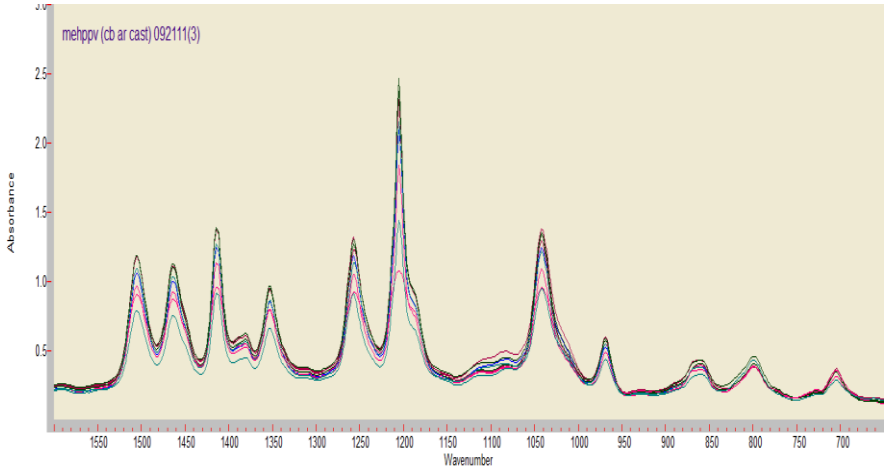

Figure 4.6: Overlay of MEH-PPV films cast from chlorobenzene under argon (1600-650cm^{-1} region)

The overlays of each film cast under different atmospheric conditions yielded no significant variation or difference in IR spectra. A representative, average spectra for each film casting condition was used for comparison. These representative spectra were overlaid for each solvent-cast film under all 3 casting atmospheres (Figure 4-7 and Figure 4-8), as well as cast under different atmospheric conditions with all 4 solvent types (Figure 4-9 and Figure 4-10). Additional IR spectra overlays can be found in the Appendix.

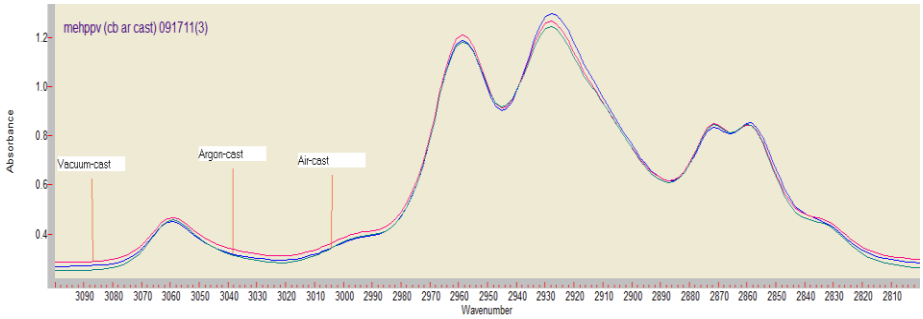

Figure 4.7: IR spectra overlay of chlorobenzene cast MEH-PPV films under vacuum, air and argon atmosphere (3100-2800cm^{-1} region)

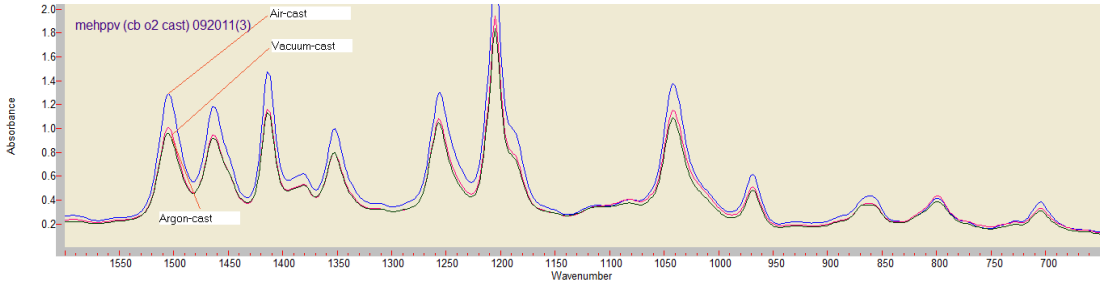

Figure 4.8: IR spectra overlay of chlorobenzene cast MEH-PPV films under vacuum, air and argon atmosphere (1600-650cm^{-1} region)

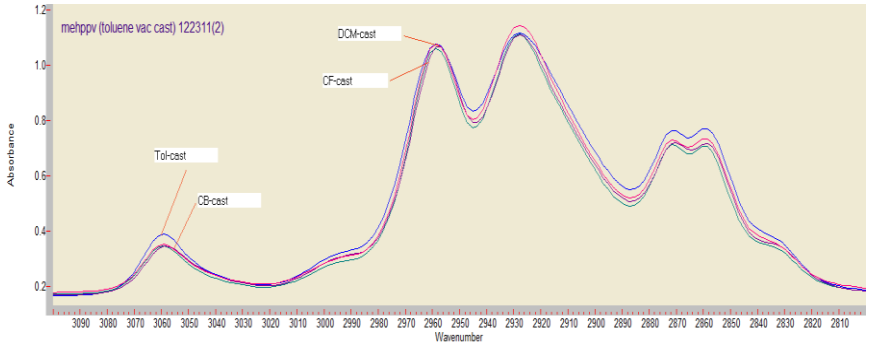

Figure 4.9: IR spectra overlay of DCM, Tol, CB and CF cast MEH-PPV films under vacuum atmosphere (3100-2800cm^{-1} region)

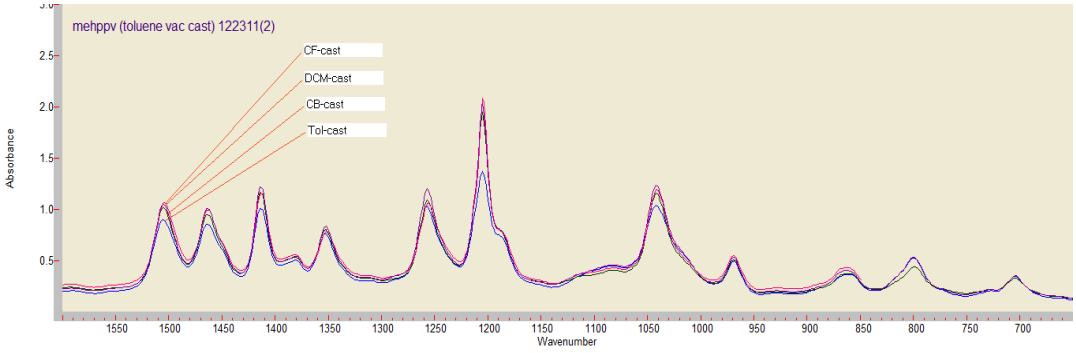

Figure 4.10: IR spectra overlay of DCM, Tol, CB and CF cast MEH-PPV films under vacuum atmosphere (3100-2800cm^{-1} region)

D. Discussion

The IR spectra of the MEH-PPV films do not show any significant shifts in the bands of interest. The MEH-PPV films showed the same IR spectra as the powder-form when overlaid (Figure 4-4). The peaks were also consistent with those assigned in the literature.[44-47] In comparison with IR spectra of the solvents used in this study, there were no additional peaks or increased intensities. The oxidation region showed weak absorptions in the baseline,

however these were not limited to a certain solvent-cast film, or atmospheric condition: these same differences were observed even within films prepared under the same conditions. The relative intensities of IR peaks between 1200- 1100 cm^{-1} were not as intense or distinct as those reported in the literature which demonstrated oxidative degradation of the polymer.[43] The oxidative degradation noted by Cumpston *et al*. [43] resulted in ester formation with new IR absorption peaks at 1740, 1290 and 1130 cm^{-1}. Further investigation into oxidative effects may be investigated in the future. For all intents and purposes, the films produced in this study were of good quality.

Yang *et al*. found in their study of MEH-PPV films differences in the intensities of some of their peaks.[29] They concluded these were surface energy differences caused by the different chain conformations in the polymer-solvent solutions carrying over into the cast film. As with many researchers they used spin-coating to prepare their samples, which is the more effective method for rapidly evaporating off the solvent and "freezing" the chain conformations from the polymer-solvent solutions in the film form. In order to produce the size and thickness films needed for this study it was not feasible at the time to use spin-casting, and the methods used (under vacuum, in argon glove bag, and fume hood) would seem to allow the polymer-solvent solution enough time to relax the polymer chains into a lower energy state with a more even conformation.

II. Fluorescence Spectroscopy

A. Introduction

Within the atoms and molecules of a sample, electrons can absorb electromagnetic radiation and become excited, pushing them to a higher energy state. Fluorescence occurs when the excited electron quickly (Average lifetime $<10^{-10}$ to 10^{-7} sec) falls back to the lower (ground) energy state. As it travels back, it emits the absorbed wavelength

from its initial excitation in the form of a photon. The study of how matter fluoresces when exposed to this energy is Fluorescence Spectroscopy.

The study of MEH-PPV films using fluorescence spectroscopy is important to gain a better understanding of how the emission band wavelengths are affected by factors such as solvent choice and casting atmosphere. Gaining an understanding of these relationships will work towards improving the efficiency and operability of the devices and displays they are used in.

Many researchers have studied the fluorescence of MEH-PPV solutions and films.[5, 11, 14, 22, 23, 29, 48, 49] The fluorescence emission (550 – 700 nm) has been found to be virtually independent of the chosen excitation wavelength; however, changes in solution concentration can have dramatic changes, with greater concentrations causing a red shift (to longer wavelengths).[11, 14, 22, 23, 29]

MEH-PPV solutions with aromatic solvents are red-shifted in comparison to aliphatic solvents, due to conformational changes by the solvent on the conjugation lengths of the emitting fluorophores.[22] In aromatic solvents, favorable π-π interactions are maximized as the polymer backbone is preferentially solvated, leading to greater conjugation lengths and a red-shift.[48] MEH-PPV films cast from aromatic solvents such as chlorobenzene also display a red-shift in the PL spectrum, a result of increased aggregation formation.[49] A decrease in the speed of spin-casting MEH-PPV films (using aromatic solvents) produces a red-shift in the PL-spectrum.[23, 29]

Aliphatic solvents possess broader emission bands than aromatics, due to preferential interaction with the side groups of MEH-PPV. This leads to several possible orientations and conformations which increase disorder.[11, 14, 22] An increase in the solvents polarity can also red shift the emission spectra of MEH-PPV slightly.[11] As the spin speed is decreased during the

casting of MEH-PPV films (aliphatic solvents) with low molecular weights, a red-shift is observed in the emission spectra; however, as the molecular weight of the polymer increases, the reverse has been observed, and a decrease in spin speed blue shifts the emission spectra.[23, 29]

MEH-PPV films cast from chloroform have exhibited a broader spectrum than toluene-cast films.[22] In general, films of MEH-PPV are red-shifted and broader than concentrated solutions.[22]

The MEH-PPV films in this study were analyzed using Fluorescence Spectroscopy to understand the relationship between casting conditions and emission band wavelength. The results of the different films were compared to each other, as well as to the literature.

B. Experimental Method

MEH-PPV films were run on a Shimadzu RF-5301PC Spectrofluorophotometer, and the results were analyzed using Panorama V3.1.32.0. An initial scan was run with excitations from 300 nm to 600 nm in 10 nm increments (Figure 4-11). The intensity of the emission band (~650 nm) increases as the excitation wavelength increases. Researchers have shown that the choice of excitation wavelength has little to no effect on the emission band wavelength: [11, 14, 22] therefore, an excitation wavelength closer to the emission band was chosen to gain an increased intensity level at the peak maxima.

Scanning Speed: Super
Response Time: Auto
Sampling Interval: 1 nm
Sensitivity: Low

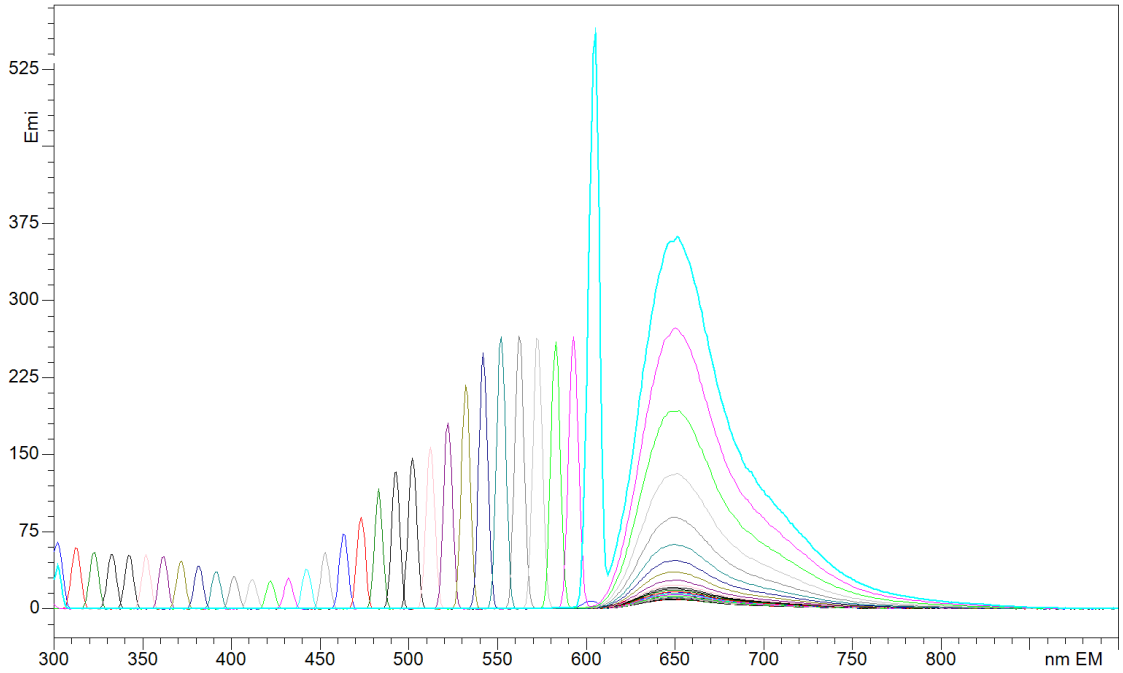

Figure 4.11: Excitation ramp from 300 nm to 600 nm in 10 nm increments of MEH-PPV film using Spectrofluorophotometer

Additional scans were conducted with optimum excitation (maximum intensity of emission) detected between 585 and 592 nm. For the purpose of this study, the excitation wavelength of 590 nm was used for comparison and analysis.

C. Experimental Results

Each MEH-PPV film-type (different casting conditions) was prepared and analyzed in triplicate on the spectrofluorophotometer. The average emission band peaks produced by the excitation wavelength at 590 nm were calculated (software) and tabulated in Table 4-2. These emission bands were overlaid (and normalized) to show comparison between different solvent-cast films under the same atmospheric conditions (Figure 4-12), as well as between the same solvent-cast films under different atmospheric casting conditions (Figure 4-13). The normalization feature in the Panorama software is used to scale the intensity values, which can be due to the small differences in the thickness of the films cast under different

conditions. All intensities of the data object are corrected using a scalar factor to fit data to the user defined borders of the new intensity interval.

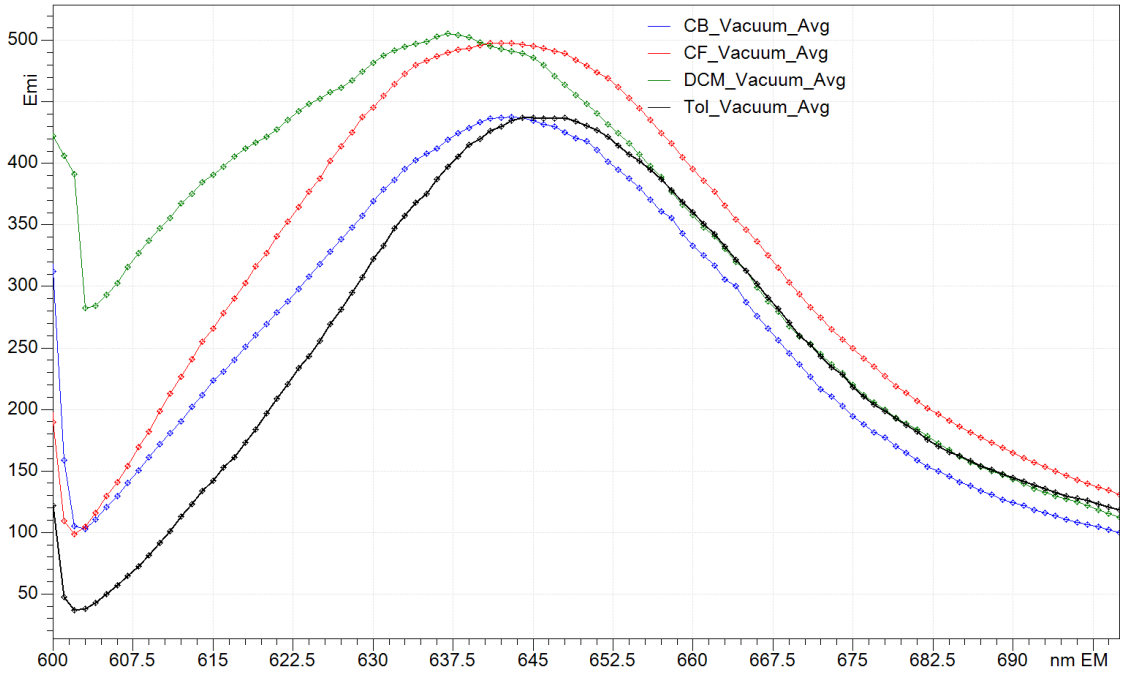

Figure 4.12: Normalized emission band overlay of (software calculated average triplicate) solvent-cast MEH-PPV films under vacuum atmosphere (using vacuum desiccator) (λ_{excit}=590 nm)

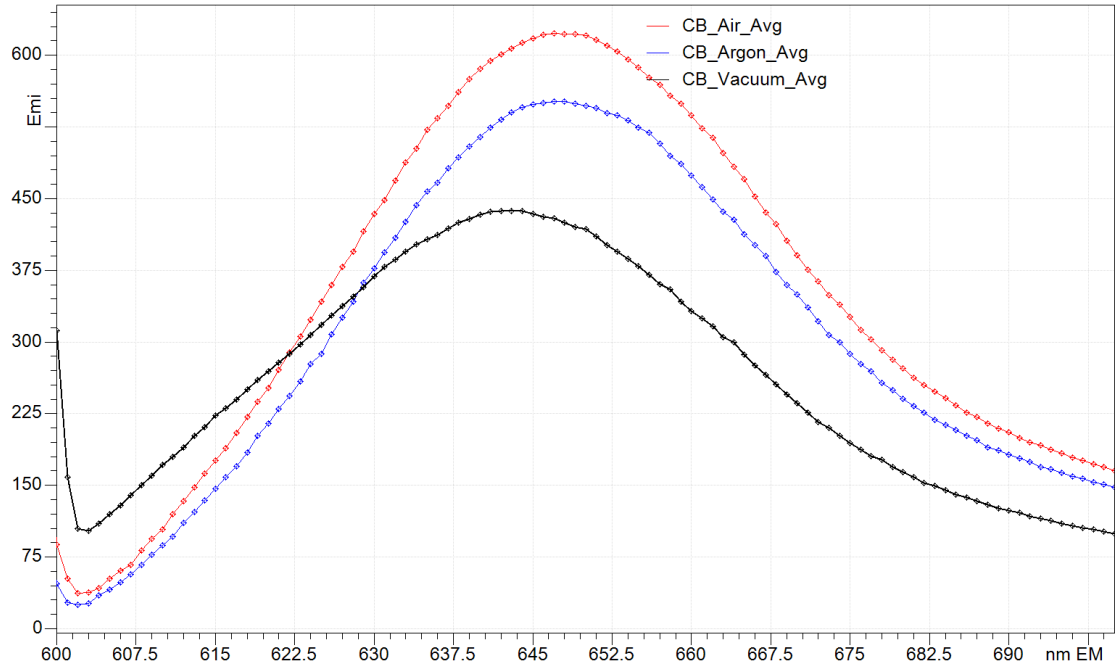

Figure 4.13: Normalized emission band overlay of (software calculated average of triplicate) chlorobenzene-cast MEH-PPV films under different atmospheric conditions (λ_{excit}=590 nm)

Solvent	Atmosphere	Avg. Emission λ (nm)
Chlorobenzene	Air	647
Chlorobenzene	Argon	647
Chlorobenzene	Vacuum	643
Toluene	Air	647
Toluene	Argon	649
Toluene	Vacuum	646
Chloroform	Air	646
Chloroform	Argon	646
Chloroform	Vacuum	641
Dichloromethane	Air	646
Dichloromethane	Argon	645
Dichloromethane	Vacuum	637

Table 4.2: Software calculated average peak emission wavelengths of triplicate MEH-PPV films using a spectrofluorophotometer (λ_{excit}=590 nm)

There is a slight red-shift in MEH-PPV films cast from aromatic solvents (chlorobenzene and toluene) compared to films cast from aliphatic solvents (chloroform and dichloromethane). Films of the same solvent-casting show little to no difference in emission peak when cast under air or argon; however there is a noticeable blue-shift of 1-9 nm when films are cast under a vacuum-atmosphere. MEH-PPV films cast from aliphatic solvents (chloroform and dichloromethane) under vacuum exhibit a broader spectrum than those films cast from aromatic solvents (chlorobenzene and toluene) under vacuum.

D. Discussion

It was reported that MEH-PPV films cast from chloroform, an aliphatic solvent, have a broader spectrum than films cast from toluene, an aromatic solvent.[22] The films in this study cast under vacuum produced the same results. Films cast from dichloromethane had broader peaks than the films cast from toluene and chlorobenzene. In summary, films cast from aliphatic solvents under vacuum exhibit a broader spectrum than films cast from aromatic solvents.

The films cast from aromatic solvents exhibit a slight red-shift compared to films cast from aliphatic solvents. This agrees with previous findings that favorable π-π interactions are maximized as the polymer backbone is preferentially solvated, leading to greater aggregation, conjugation lengths, and a red-shift in solution.[48]

To date there has been no known studies done on how the atmospheric conditions under which the MEH-PPV films are cast affects fluorescence. The results of this study show a blue-shift of 1-9 nm in films cast under vacuum atmosphere, when compared to those cast under air or argon. A possible explanation is that solvents take longer to evaporate when cast under air and argon, as opposed to vacuum which speeds the process. A decrease in the speed of spin-casting MEH-PPV films (using aromatic solvents) produces a red-shift in the PL-spectrum.[23, 29] Slow solvent evaporation of the films should favor entanglement of the polymer chains: this leads to the formation of stronger aggregates (known to promote luminescent properties), which in turn should favor the formation of interchain species.[23] An increase in the number of aggregates present in the MEH-PPV film has been shown to promote a red-shift in the PL spectrum.[49]

III. Spectroscopy Summary

MEH-PPV films can be easily processed onto different substrates that are useful in novel devices.[4] Such devices include plastic light-emitting diodes (LED),[4, 6] and flexible displays.[5] Both of these devices involve the use of radiated energy, which makes the spectroscopic study of MEH-PPV films important.

The study of MEH-PPV films using fluorescence spectroscopy is important to gain a better understanding of how the emission band wavelengths are affected by factors such as solvent choice and casting atmosphere. Gaining an understanding of these relationships will work towards improving the efficiency and operability of the devices and displays they are used

in. Many researchers have studied the fluorescence of MEH-PPV solutions and films. [5, 11, 14, 22, 23, 29, 48, 49] The fluorescence emission (550 – 700 nm) has been found to be virtually independent of the chosen excitation wavelength.[11, 14, 22]

In this study of MEH-PPV, films cast from aliphatic solvents under a vacuum atmosphere exhibited a broader spectrum than films cast from aromatic solvents. This correlation is supported by previous results of Cossiello *et al.*[22] that chloroform-cast films exhibited a broader spectra than MEH-PPV toluene-cast films. The films cast from aromatic solvents exhibited a slight red-shift compared to films cast from aliphatic solvents. This agrees with previous findings that favorable π-π interactions are maximized as the polymer backbone is preferentially solvated, leading to greater conjugation lengths and a red-shift in solution.[48] To date there has been no known studies done on how the atmospheric conditions under which the MEH-PPV films are cast affects fluorescence. The results of this study show a blue-shift of 1-9 nm in films cast under vacuum atmosphere, when compared to those under air and argon. A possible explanation is that solvents take longer to evaporate when cast under air and argon, as opposed to vacuum which speeds the process. Slow solvent evaporation of the films should favor entanglement of the polymer chains: this leads to the formation of stronger aggregates (known to promote luminescent properties), which in turn should favor the formation of interchain species.[23] An increase in the number of aggregates present in the MEH-PPV film has been shown to promote a red-shift in the PL spectrum.[49]

The IR spectra of the MEH-PPV films in this study did not show any significant shifts in the bands of interest. The MEH-PPV films showed the same IR spectra as the powder-form when overlaid. The peaks were also consistent with those assigned in the literature.[44-47] In comparison with IR spectra of the solvents used in this study, there were no additional peaks or

increased intensities. The films produced in this study consisted of MEH-PPV with no evident contaminants.

Future Work

The work done in this study was another step forward in understanding how film preparation and processing affects the morphology of MEH-PPV films. Results from each aspect of the study can be correlated and/or verified by previous work done by other researchers. Some of the work done varying the atmospheric casting conditions and comparing the corresponding property changes shows promise as being a preparatory method that should be strongly considered along with solvent choice for groups interested in using these (or similar) films going forward.

The results of this study should serve as a strong foundation for a second phase in this line of study. Phase II would involve adding two more aromatic and aliphatic solvents to study, preferably ones found in literature for comparison. Films will be stored in different atmospheric conditions (argon box, ambient room conditions, and direct sun/window) and analyzed over the course of 1 year (3-month intervals) to observe the degradative effects over time. Spin-casting of the films is a common method used in the literature, however it does not traditionally produce the pristine quality films used throughout this study. This is an important consideration when doing mechanical and thermal analysis, however for comparison purposes the method would have to be practiced and performed as carefully and controlled as possible.

The use of a DMA with sub-ambient capabilities would add the benefits of mechanical properties, as well as more accurate T_g temperatures. X-ray diffraction (XRD) studies on MEH-PPV films cast from THF exhibited a higher degree of anisotropy of chain orientation with respect to the substrate, as well as a higher degree of crystallinity and larger crystalline domains than films cast from CB or p-xylene.[21] Films cast from chloroform exhibit a lower

degree of crystallinity than films cast from toluene.[22] X-ray diffraction (XRD) could be beneficial to the comparison of crystallinity and thermal properties, even though MEH-PPV films are known to possess low degrees of crystallinity (which make analysis sometimes difficult).

Preliminary tests were performed on a thermogravimetric analyzer (TGA) to observe the effects of morphology and casting conditions on the decomposition and thermal stability of the polymer. Future studies will investigate this further, as well as the activation energies of these step losses, and lifetime prediction calculations of the polymer film at different temperatures.

Finally, future studies will involve dynamic infrared spectroscopy. This technique involves putting a constant perturbation on the polymer film, and recording the IR spectra as the sample stretches and relaxes. This leads to the understanding of the elastic and viscous orientation behavior of the polymer under conditions under a dynamic strain, and can provide insight into the bands and chains that are active as the polymer backbone is stretched.

Appendix

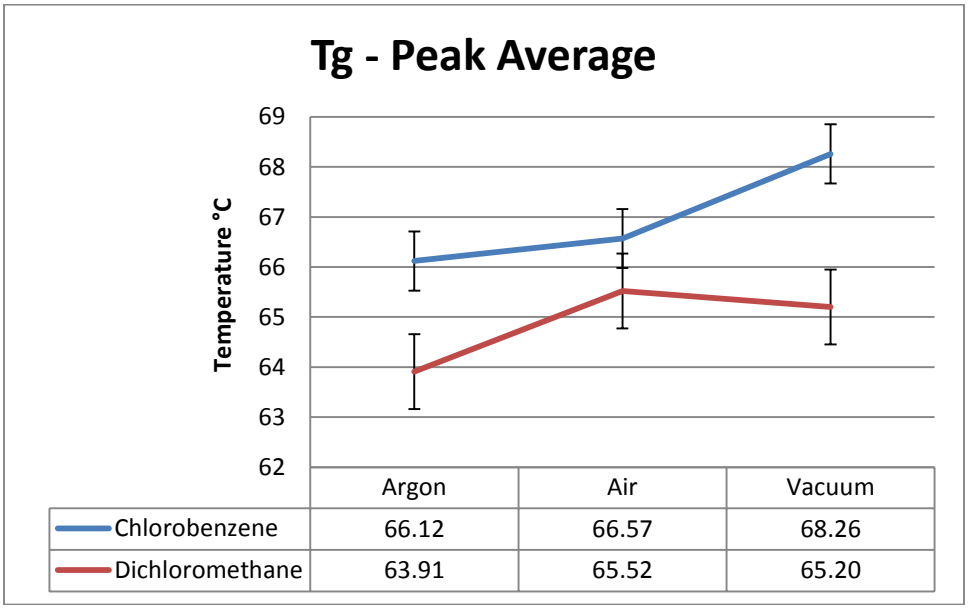

Figure A-1. Average DSC T_g measurements for CB and DCM cast films using the peak of the transition curve (with average standard deviation)

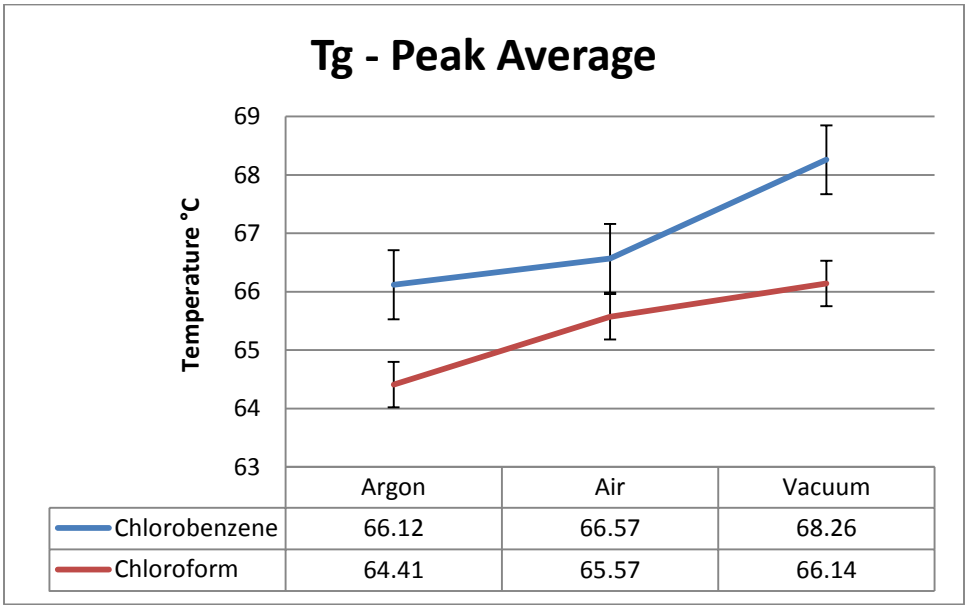

Figure A-2. Average DSC T_g measurements for CB and CF cast films using the peak of the transition curve (with average standard deviation)

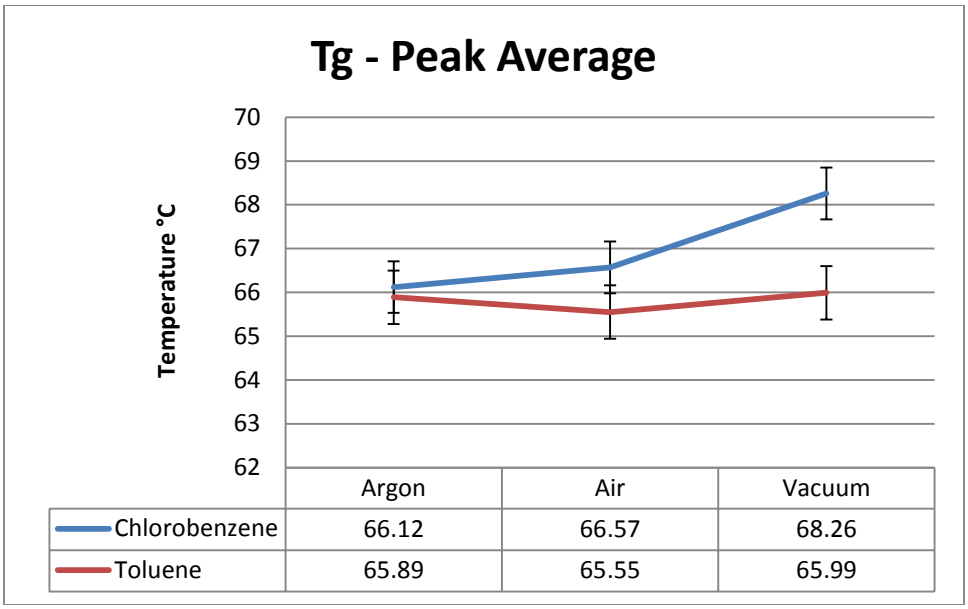

Figure A-3. Average DSC T_g measurements for CB and Toluene cast films using the peak of the transition curve (with average standard deviation)

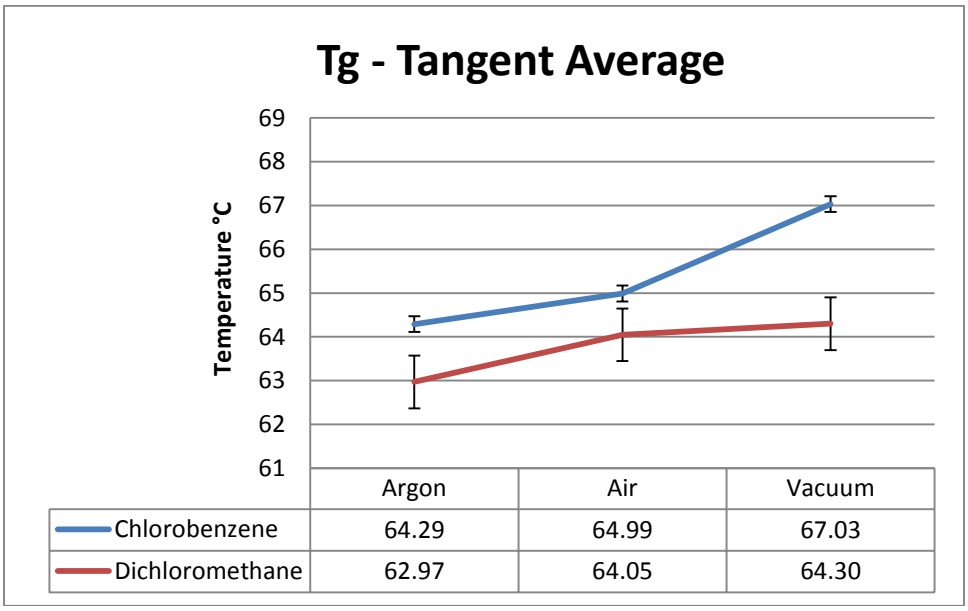

Figure A-4. Average DSC T_g measurements for CB and DCM cast films using lines tangent to the transition curve (with average standard deviation)

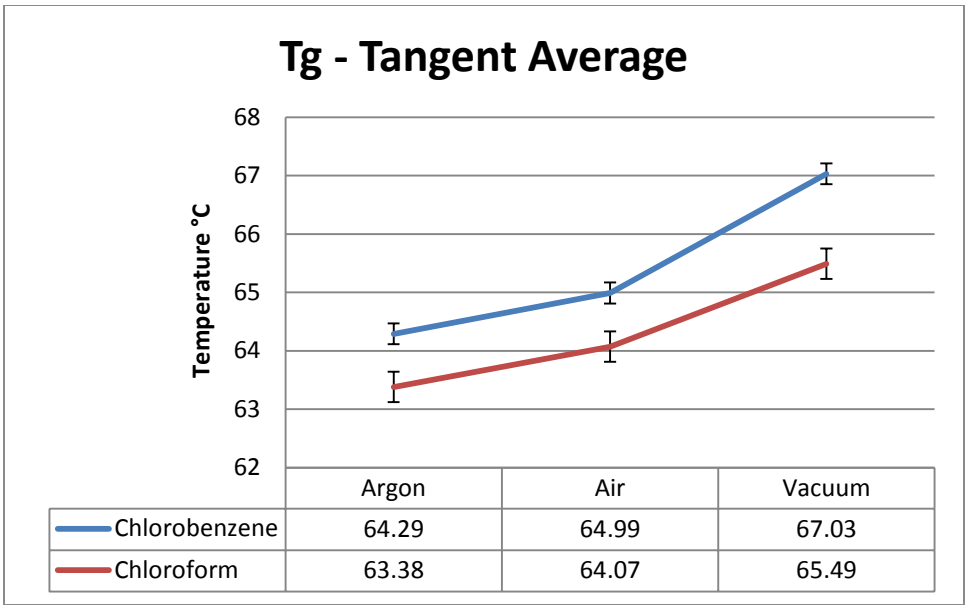

Figure A-5. Average DSC T_g measurements for CB and CF cast films using lines tangent to the transition curve (with average standard deviation)

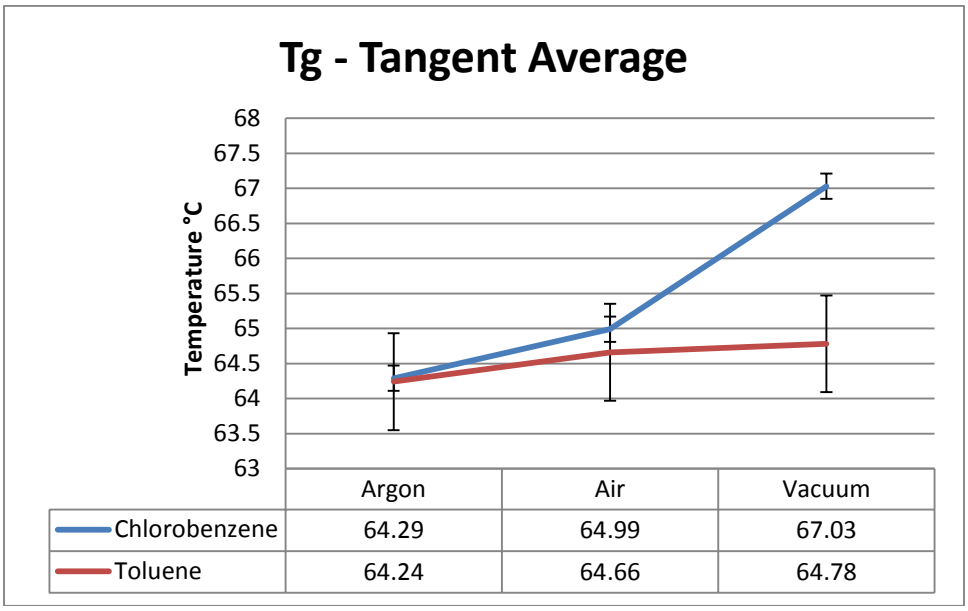

Figure A-6. Average DSC T_g measurements for CB and toluene cast films using lines tangent to the transition curve (with standard deviation)

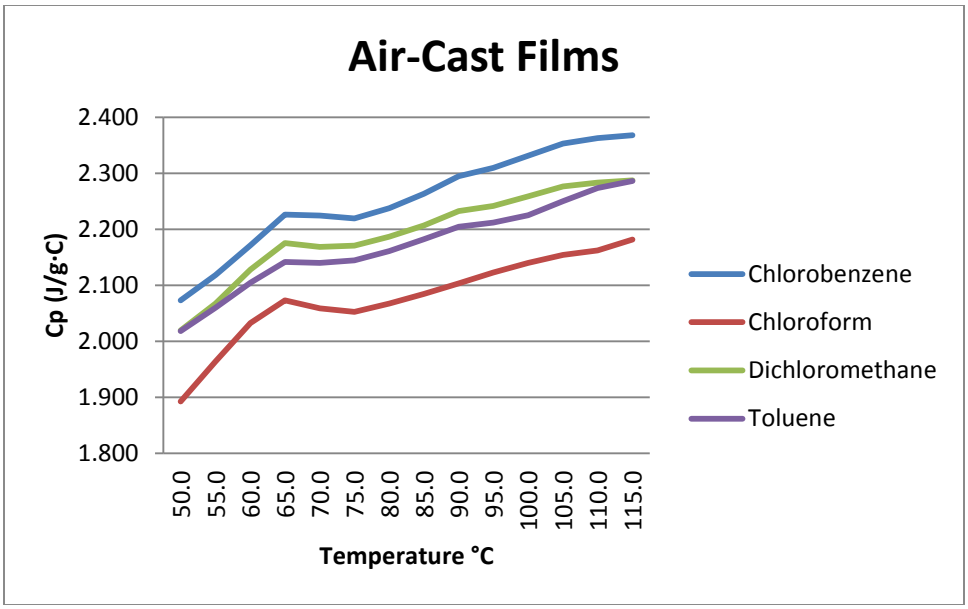

Figure A-7. Overlay of average DSC C_p measurements for air-cast films (using different solvents)

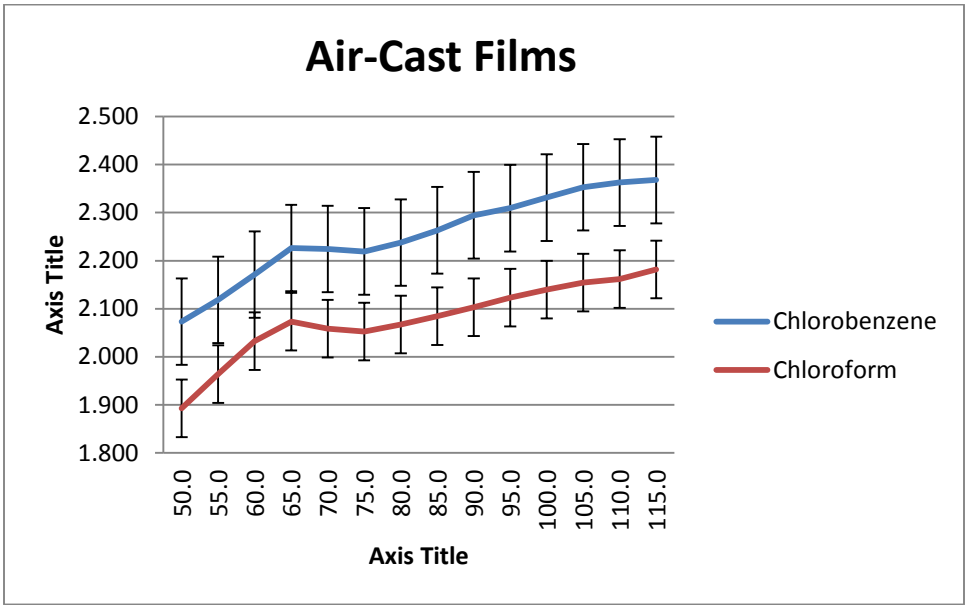

Figure A-8. Overlay of average DSC C_p measurements for air-cast films (using chlorobenzene and chloroform) with standard deviations noted

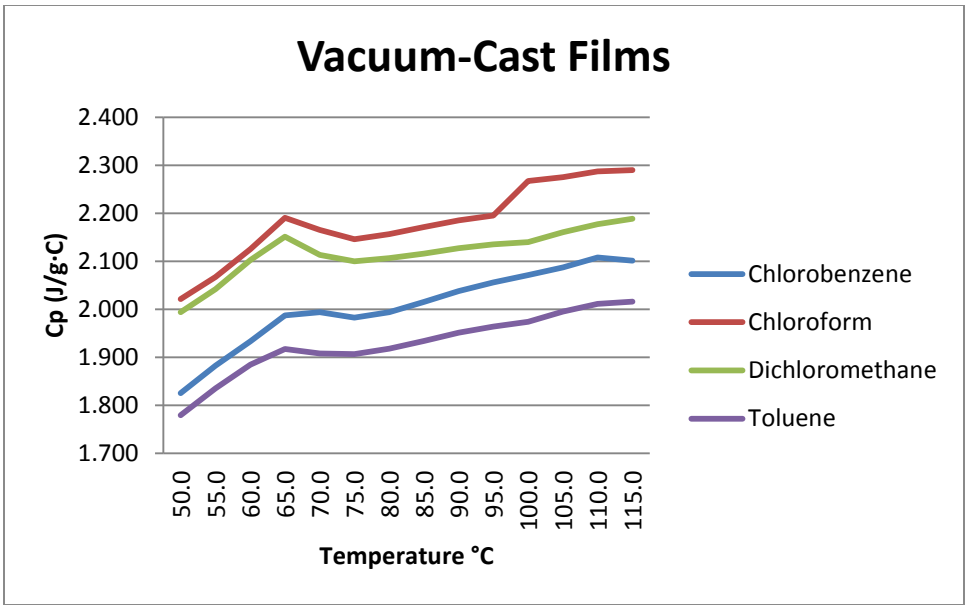

Figure A-9. Overlay of average DSC C_p measurements for vacuum-cast films (using different solvents)

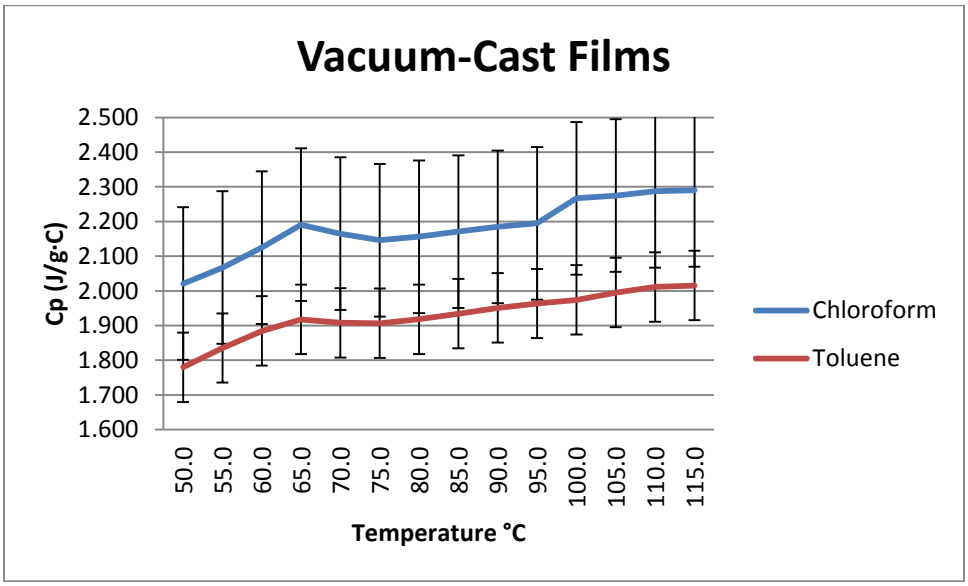

Figure A-10. Overlay of average DSC C_p measurements for vacuum-cast films (using chloroform and toluene) with standard deviations noted

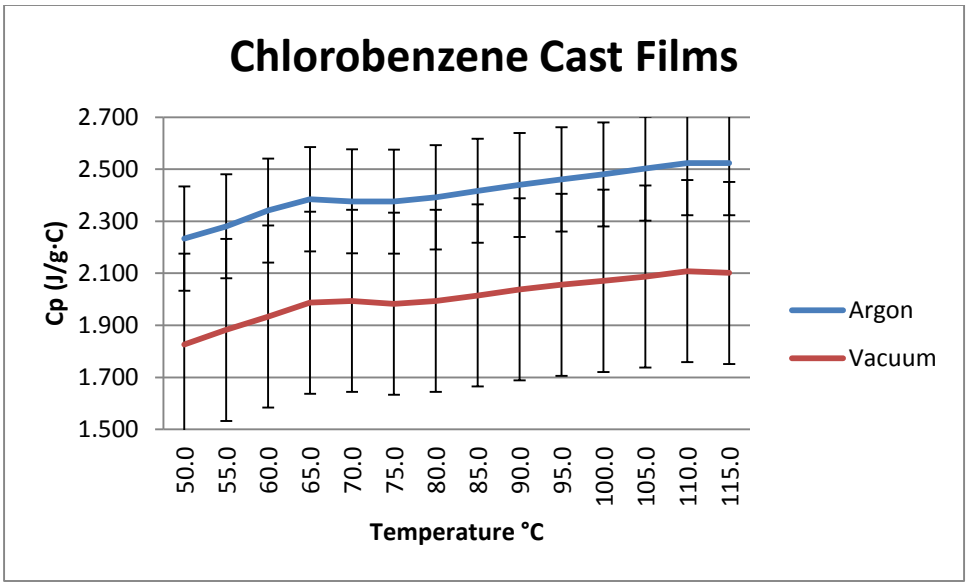

Figure A-11. Overlay of average DSC C_p measurements for chlorobenzene-cast films (under argon and vacuum) with standard deviations noted

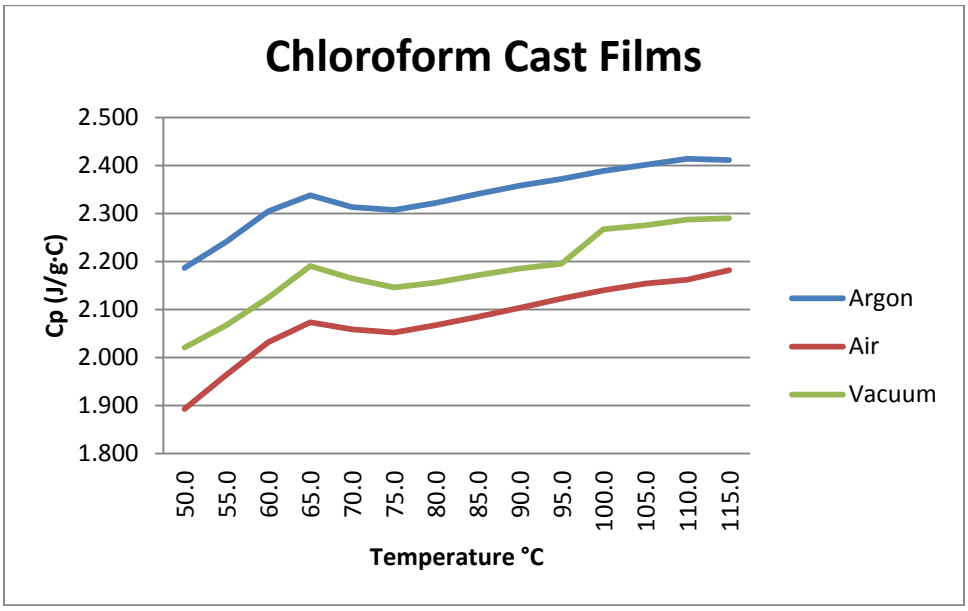

Figure A-12. Overlay of average DSC C_p measurements for chloroform-cast films (under different atmospheres)

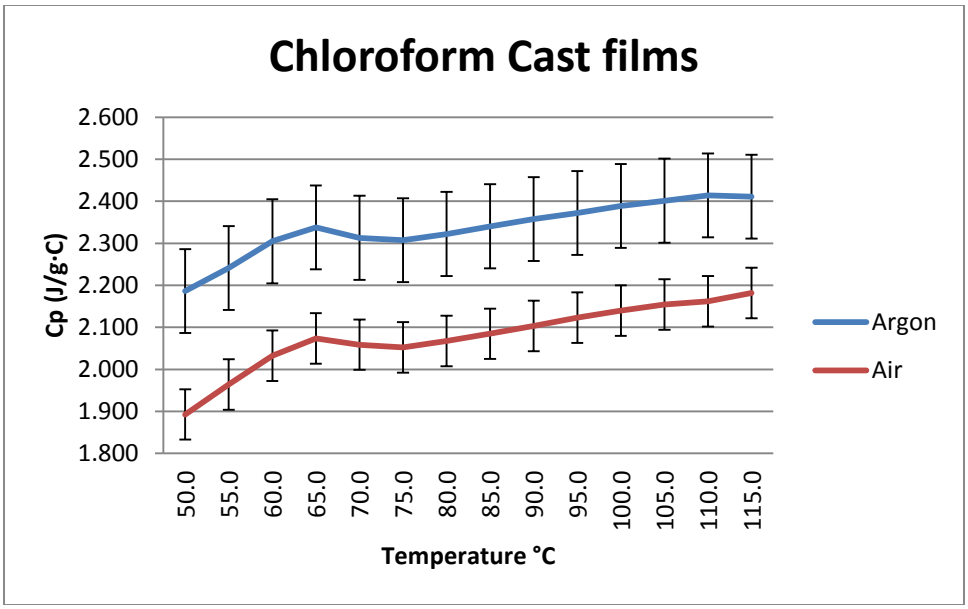

Figure A-13. Overlay of average DSC C_p measurements for chloroform-cast films (under argon and air) with standard deviations noted

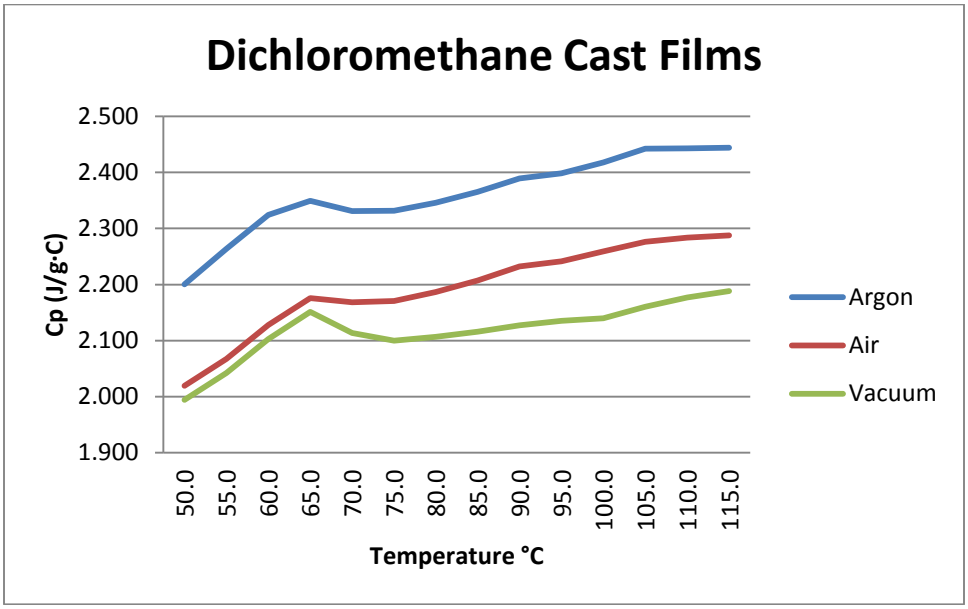

Figure A-14. Overlay of average DSC C_p measurements for dichloromethane-cast films (under different atmospheres)

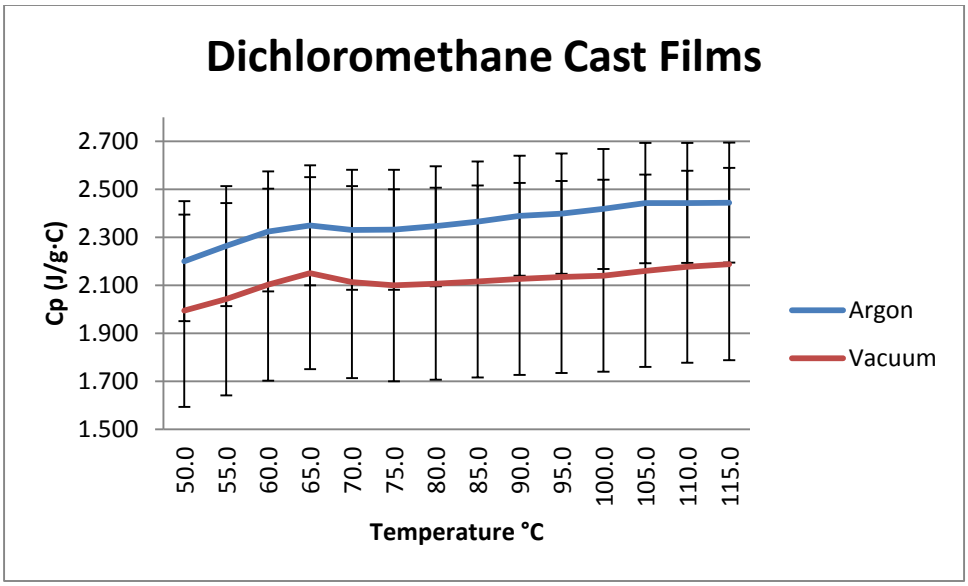

Figure A-15. Overlay of average DSC C_p measurements for dichloromethane-cast films (under argon and vacuum) with standard deviations noted

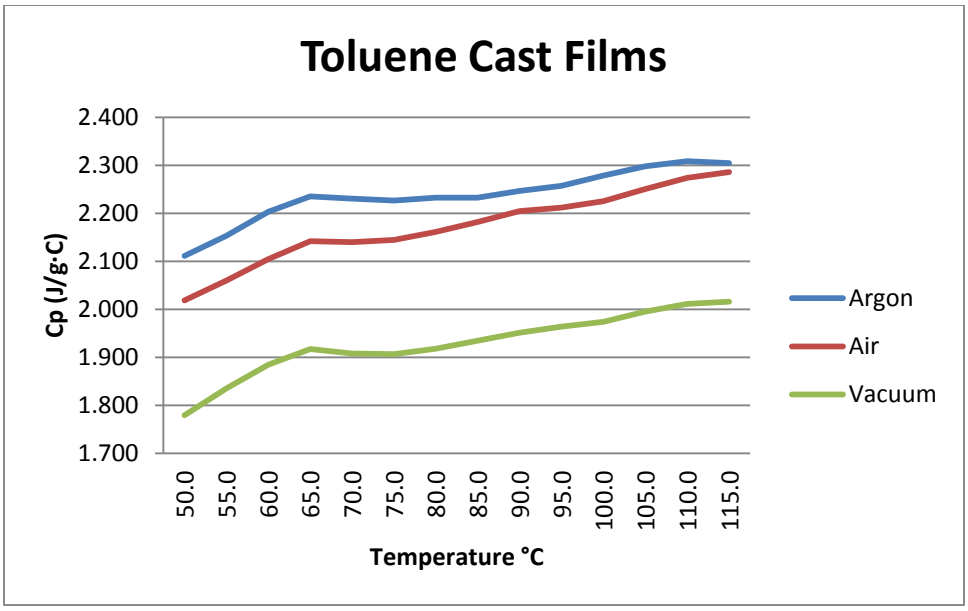

Figure A-16. Overlay of average DSC C_p measurements for toluene-cast films (under different atmospheres)

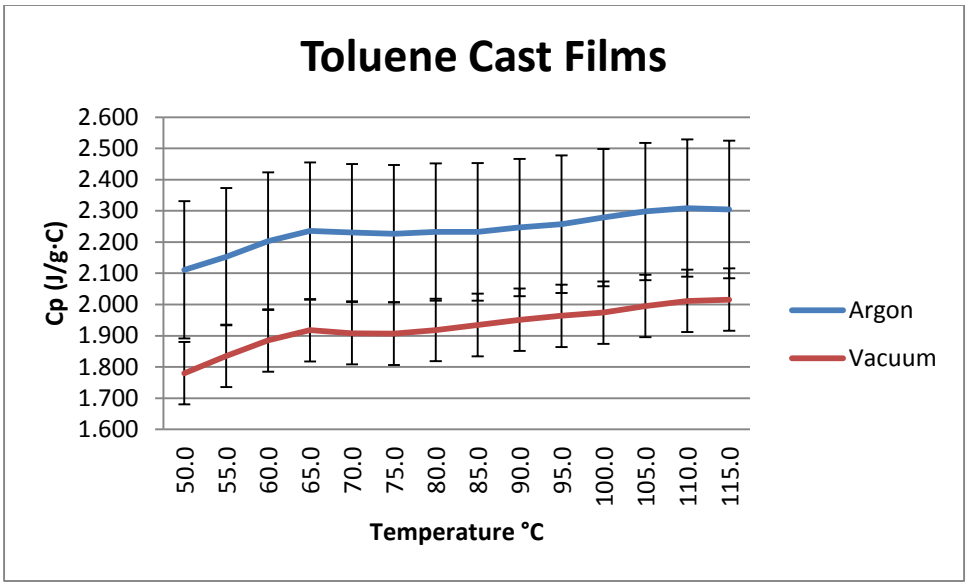

Figure A-17. Overlay of average DSC C_p measurements for toluene-cast films (under argon and vacuum) with standard deviations noted

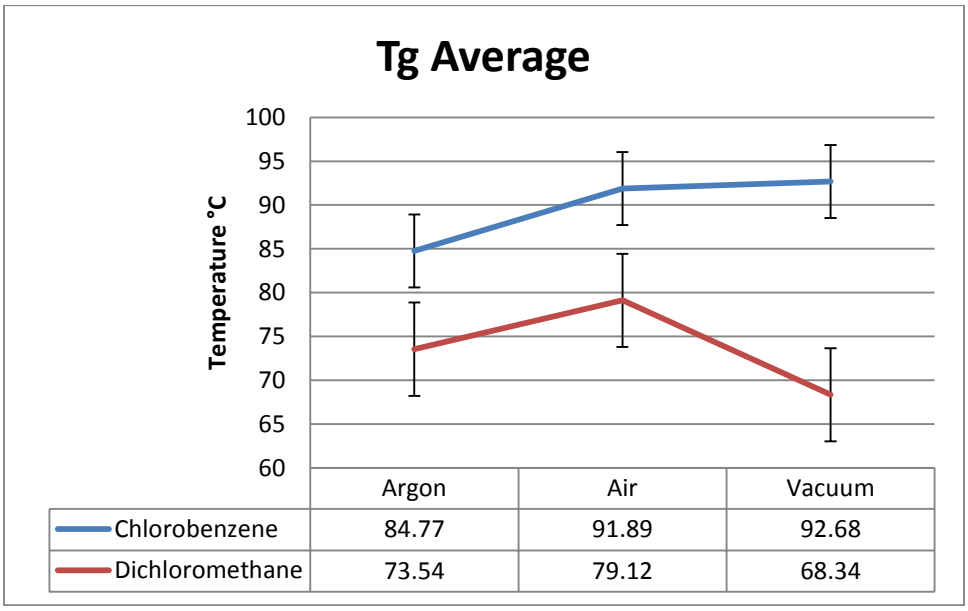

Figure A-18. Overlay of average DMA T_g measurements for chlorobenzene and dichloromethane cast films with standard deviations noted

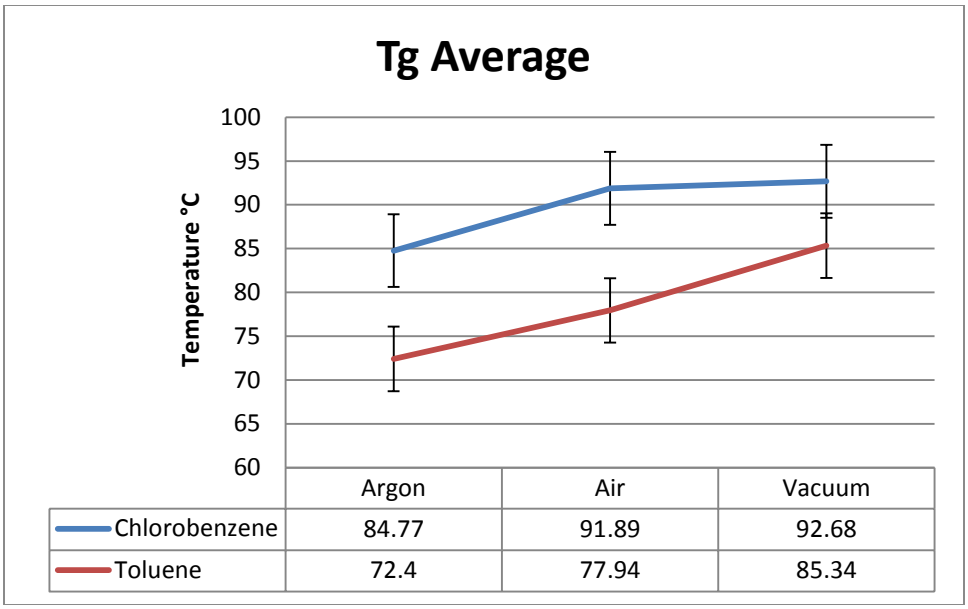

Figure A-19. Overlay of average DMA T_g measurements for chlorobenzene and toluene cast films with standard deviations noted

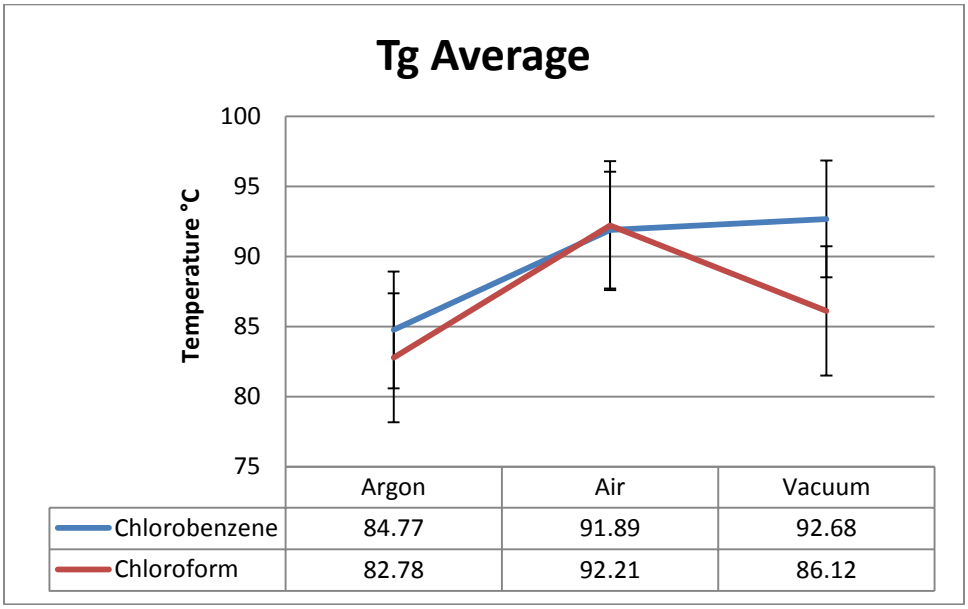

Figure A-20. Overlay of average DMA T_g measurements for chlorobenzene and chloroform cast films with standard deviations noted

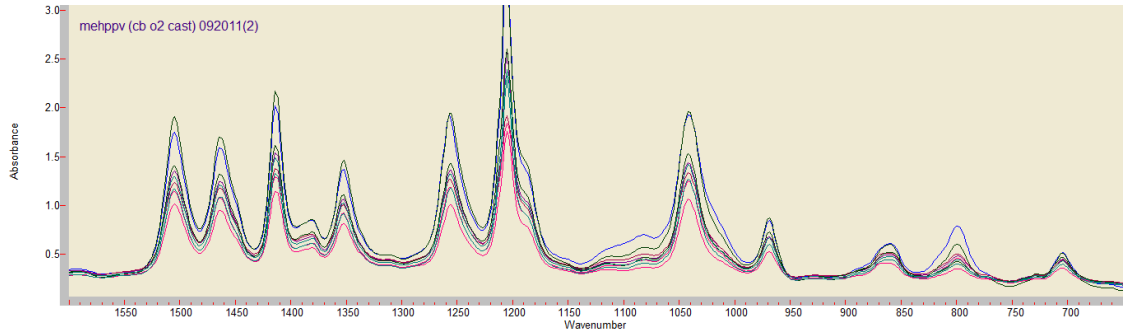

Figure A-21. IR-spectra overlay of MEH-PPV films cast with chlorobenzene under air atmosphere.

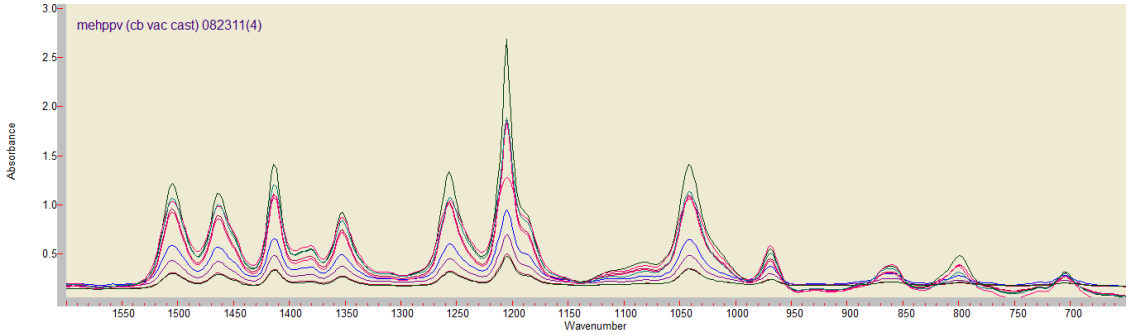

Figure A-22. IR-spectra overlay of MEH-PPV films cast with chlorobenzene under vacuum.

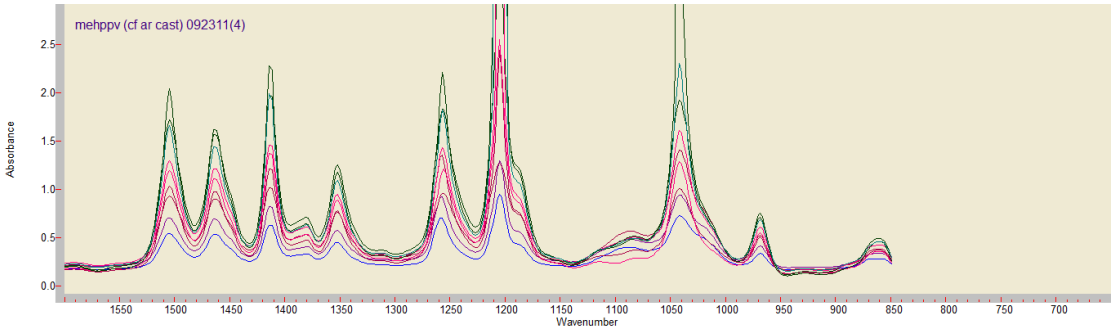

Figure A-23. IR-spectra overlay of MEH-PPV films cast with chloroform in argon

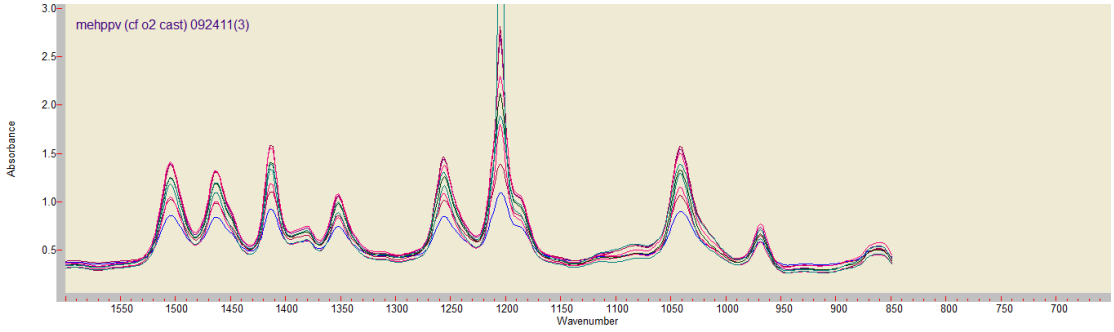

Figure A-24. IR-spectra overlay of MEH-PPV films cast with chloroform under air atmosphere

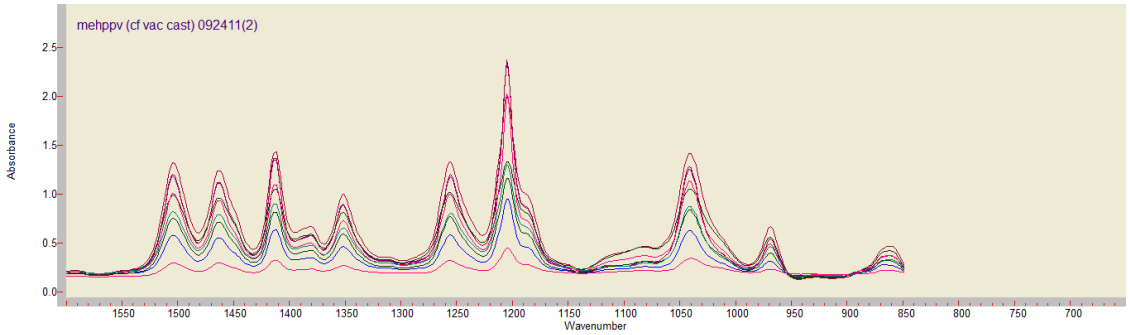

Figure A-25. IR-spectra overlay of MEH-PPV films cast with chloroform under vacuum

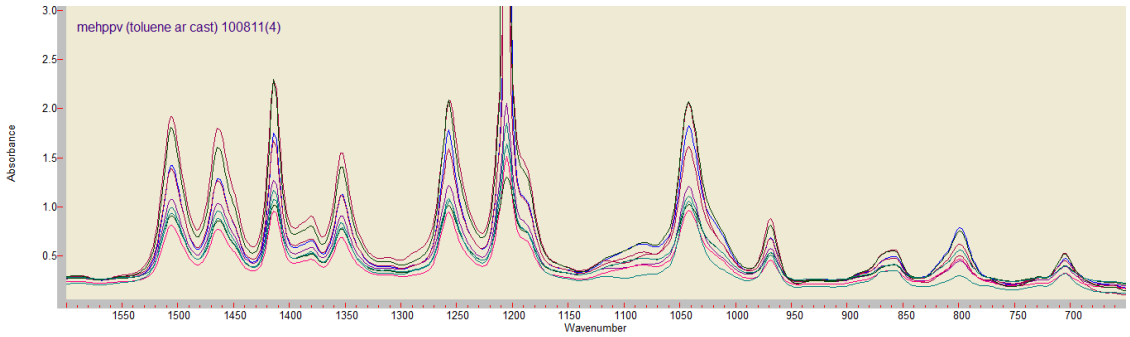

Figure A-26. IR-spectra overlay of MEH-PPV films cast with toluene in argon

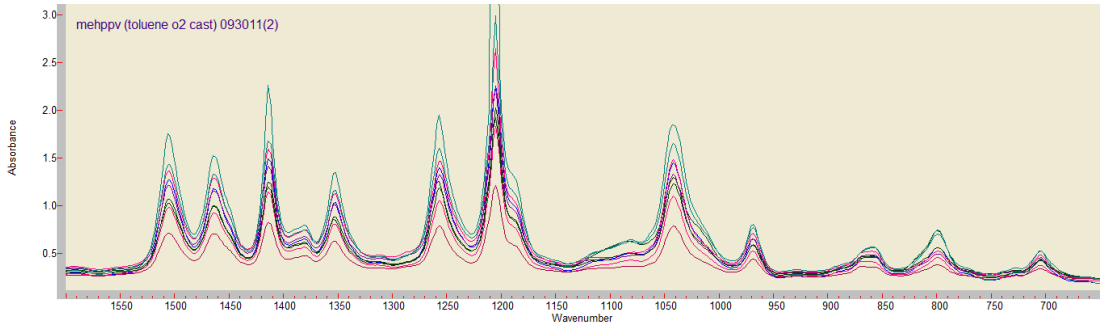

Figure A-27. IR-spectra overlay of MEH-PPV films cast with toluene under air atmosphere

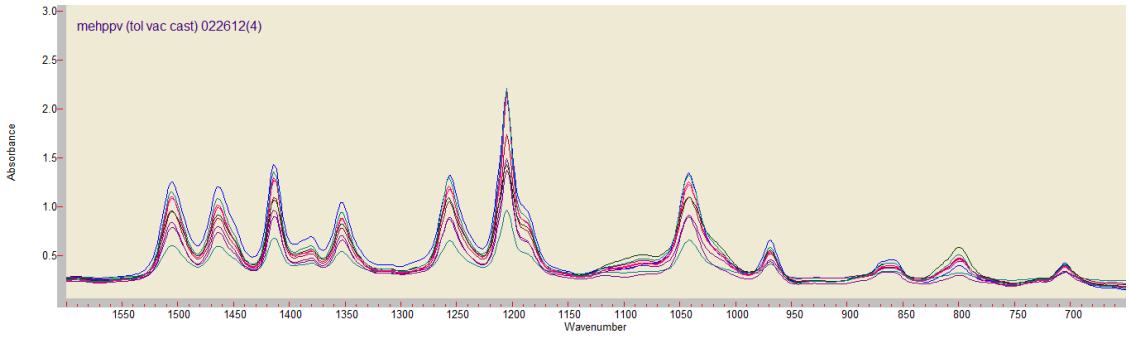

Figure A-28. IR-spectra overlay of MEH-PPV films cast with toluene under vacuum

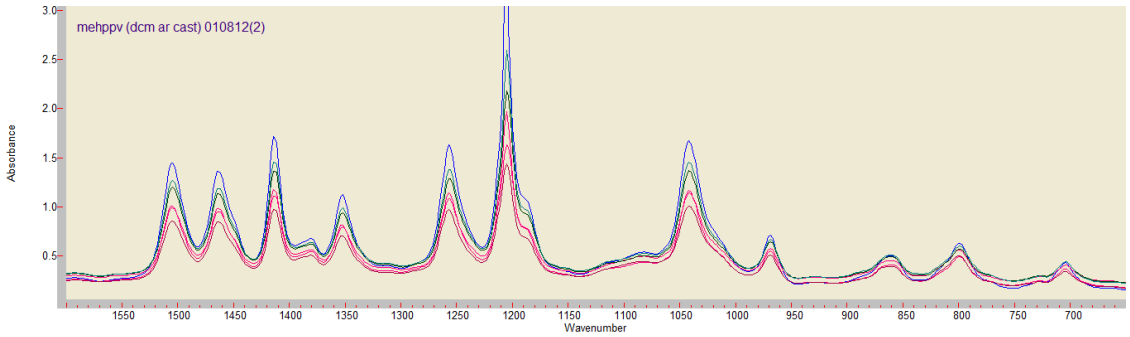

Figure A-29. IR-spectra overlay of MEH-PPV films cast with dichloromethane in argon

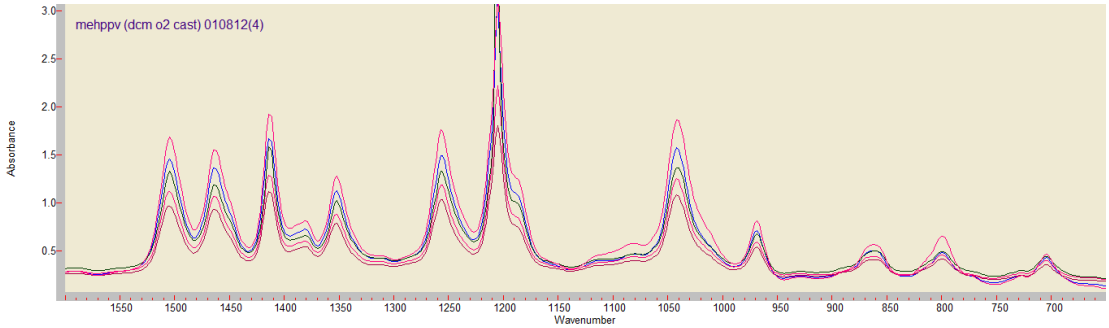

Figure A-30. IR-spectra overlay of MEH-PPV films cast with dichloromethane under air atmosphere

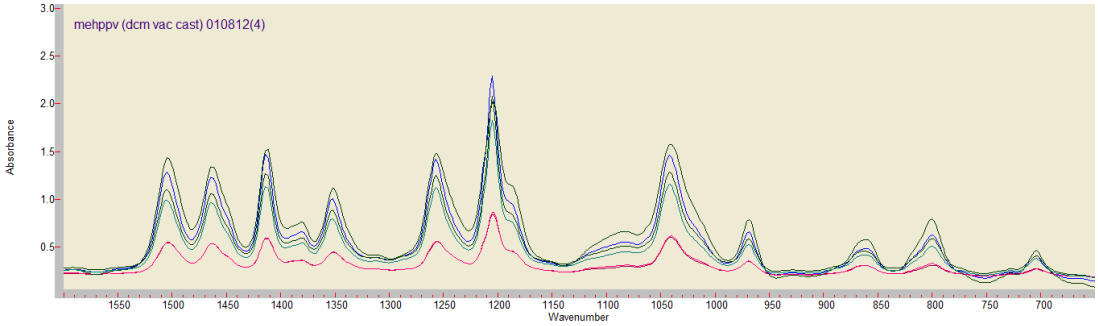

Figure A-31. IR-spectra overlay of MEH-PPV films cast with dichloromethane under vacuum

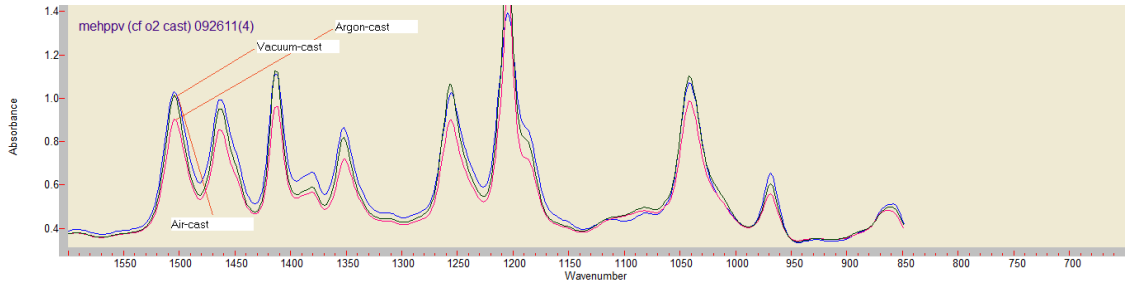

Figure A-32. IR-spectra overlay of chloroform cast MEH-PPV films under vacuum, air and argon atmosphere

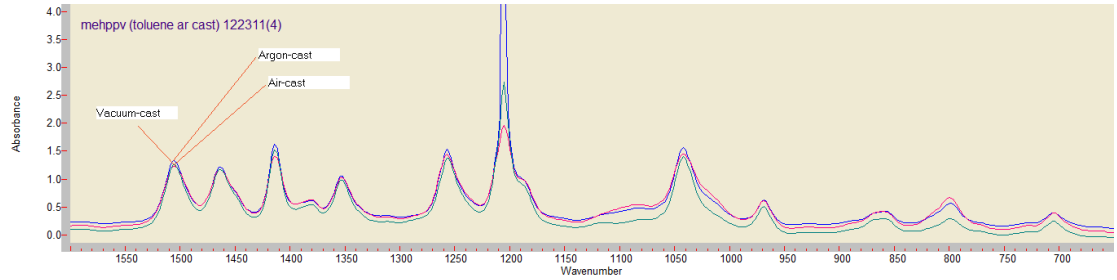

Figure A-33. IR-spectra overlay of toluene cast MEH-PPV films under vacuum, air and argon atmosphere.

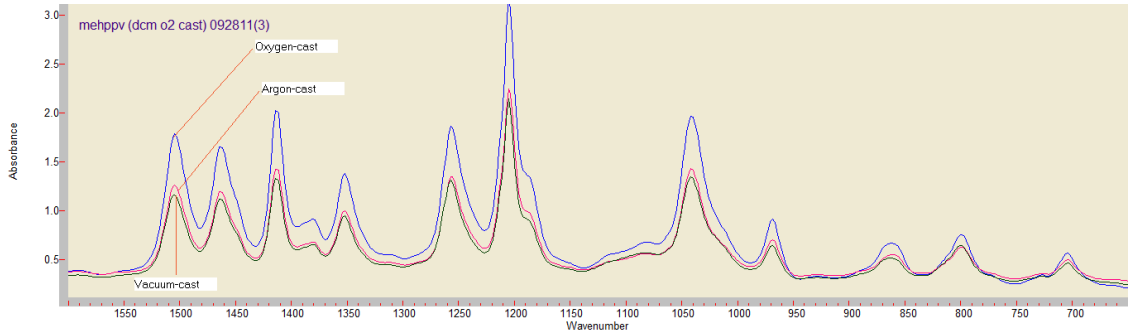

Figure A-34. IR-spectra overlay of dichloromethane cast MEH-PPV films under vacuum, air and argon atmosphere

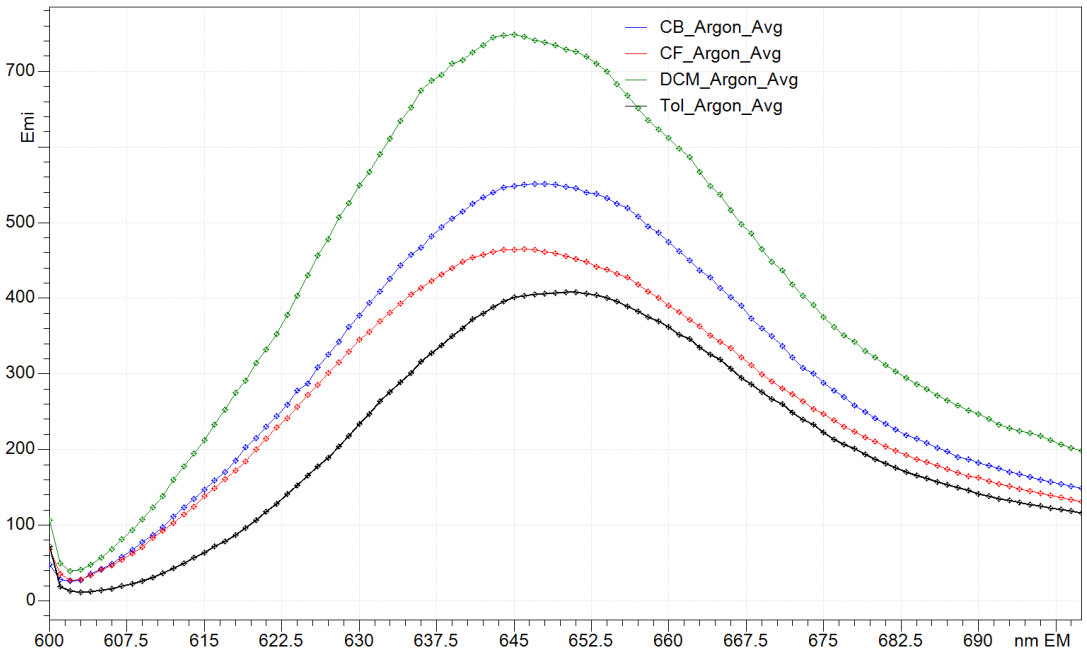

Figure A-35: Normalized emission band overlay of (average) solvent-cast MEH-PPV films under argon atmosphere (λ_{excit}=590 nm)

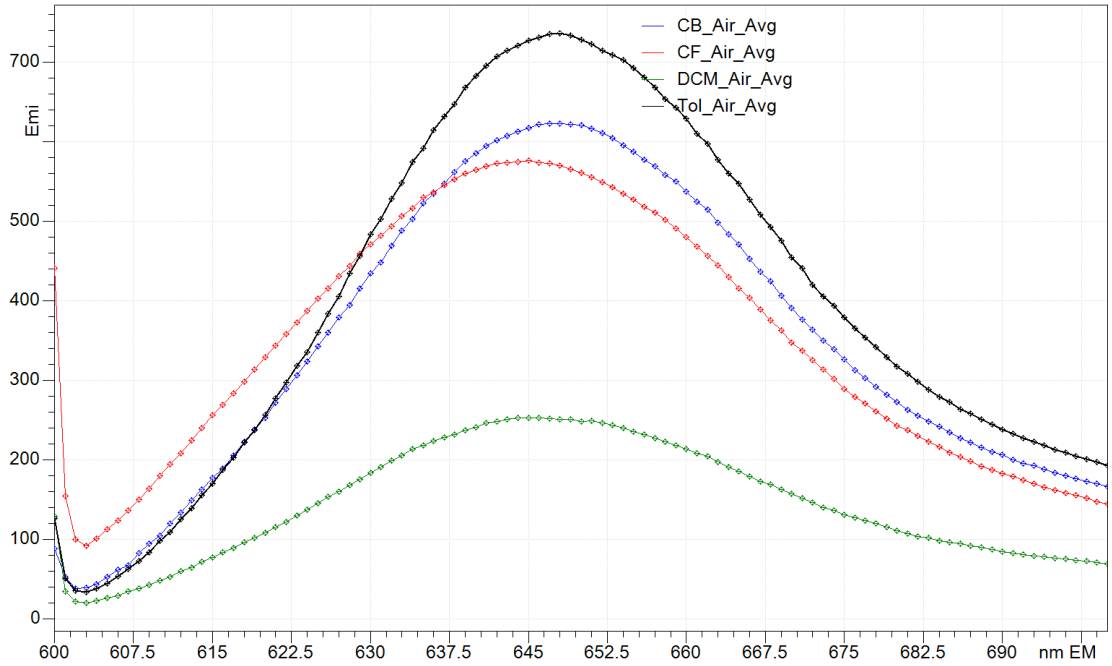

Figure A-36: Normalized emission band overlay of (average) solvent-cast MEH-PPV films under air atmosphere (λ_{excit}=590 nm)

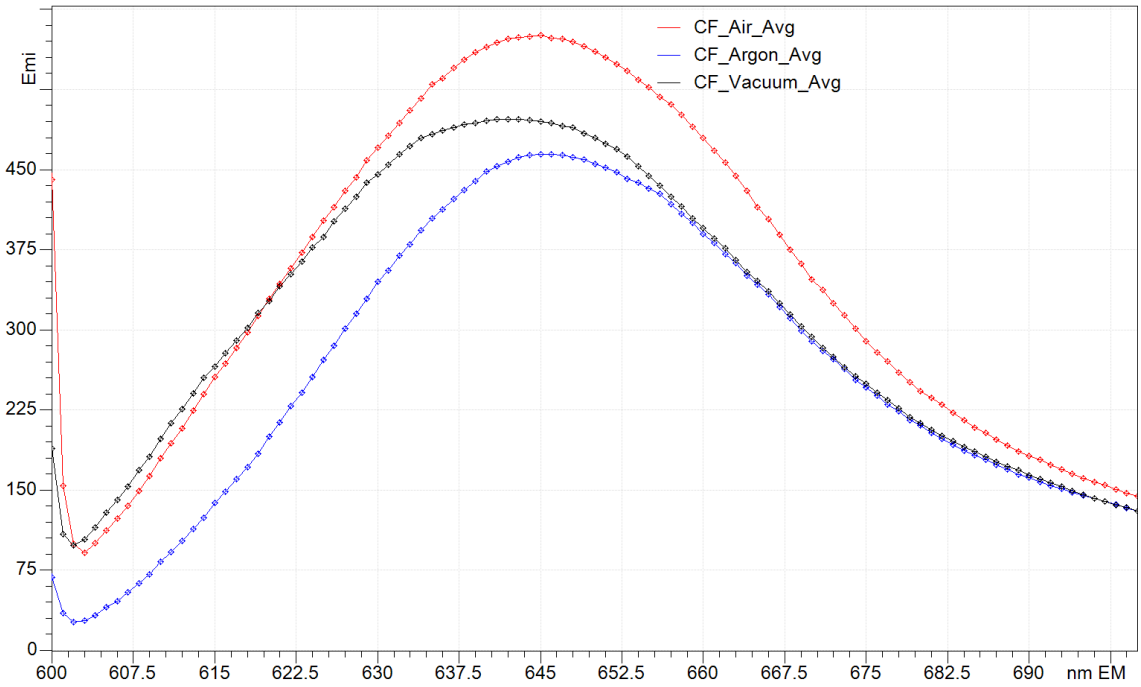

Figure A-37: Normalized emission band overlay of (average) chloroform-cast MEH-PPV films under different atmospheric conditions (λ_{excit}=590 nm)

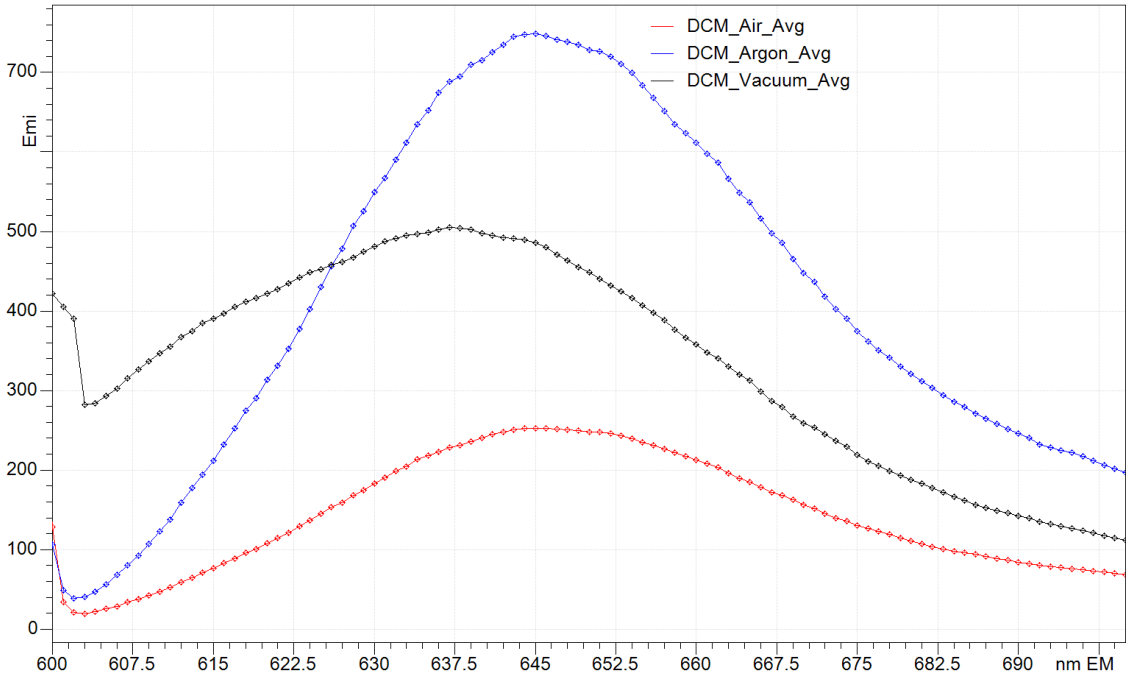

Figure A-38: Normalized emission band overlay of (average) dichloromethane-cast MEH-PPV films under different atmospheric conditions (λ_{excit}=590 nm)

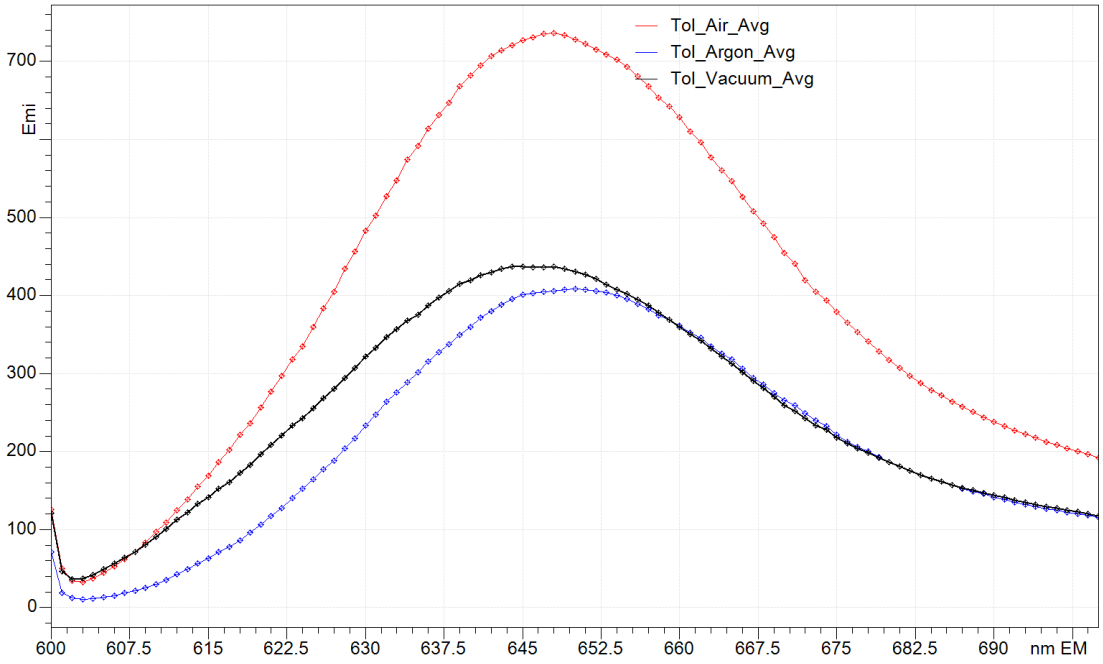

Figure A-39: Normalized emission band overlay of (average) toluene-cast MEH-PPV films under different atmospheric conditions (λ_{excit}=590 nm)

References

1. Friend RH, Gymer RW, Holmes AB, Burroughes JH, Marks RN, Taliani C, Bradley DDC, Dos Santos DA, Bredas JL, Logdlund M, *et al.* Electroluminescence in conjugated polymers. Nature 1999;397:121-128.

2. Kraft A, Gramisdale AC, Holmes AB. Electroluminescent conjugated polymers-seeing polymers in a new light. Angewandte Chemie International English Edition 1998;37:402-428.

3. Braun D, Heegar AJ. Visible light emission from semiconducting polymer diodes. Applied Physics Letters. 1991;58:1982-1984.

4. Gustafsson G, Cao Y, Treacy GM, Klavetter F, Colaneri N, Heeger AJ. Flexible light-emitting diodes made from soluble conducting polymers. Nature 1992;357:477-479.

5. Schwartz BJ. Conjugated polymers as molecular materials: How chain conformation and film morphology influence energy transfer and interchain interactions. Annual Review of Physical Chemistry 2003;54:141-172.

6. Burroughes JH, Bradley DDC, Brown AR, Marks RN, Mackay K, Friend RH, Burns PL, Holmes AB. Light-emitting diodes based on conjugated polymers. Nature 1990;347:539-541.

7. Brabec CJ, Sariciftci NS, Hummelen JC. Plastic solar cells. Advanced Functional Materials 2001;11:15-26.

8. Huitema HEA, Gelinck GH, Van DP, Kuijk KE, Hart CM, Cantatore E, Herwig PT, Van Breemen, A. J. J. M., De Leeuw DM. Plastic transistors in active-matrix displays. Nature 2001;414:599-599.

9. Tang CW, VanSlyke SA. Organic electroluminescent diodes. Applied Physics Letters. 1987;51:913-915.

10. Reshak AH, Shahimin MM, Juhari N, Suppiah S. Electrical behaviour of MEH-PPV based diode and transistor. Progress in Biophysics and Molecular Biology 2013;113:289-294.

11. Zheng M, Bai F, Zhu D. Photophysical process of MEH-PPV solution. Journal of Photochemistry and Photobiology A: Chemistry 1998;116:143-145.

12. Nguyen T, Yee RY, Schwartz BJ. Solution processing of conjugated polymers: The effects of polymer solubility on the morphology and electronic properties of semiconducting polymer films. Journal of Photochemistry and Photobiology A: Chemistry 2001;144:21-30.

13. Nguyen T, Doan V, Schwartz BJ. Conjugated polymer aggregates in solution: Control of interchain interactions. Journal of Chemical Physics 1999;110:4068-4078.

14. Quan S, Teng F, Xu Z, Qian L, Hou Y, Wang Y, Xu X. Solvent and concentration effects on fluorescence emission in MEH-PPV solution. European Polymer Journal 2006;42:228-233.

15. Wang P, Wu LL, Zhang D, Zhang HQ. Effect of chain conformation on micro-mechanical behaviour of MEH-PPV thin film. Bulletin of Materials Science 2013;36:833-837.

16. Nguyen T, Martini IB, Liu J, Schwartz BJ. Controlling interchain interactions in conjugated polymers: The effects of chain morphology on exciton-exciton annihilation and aggregation in MEH-PPV films. Journal of Physical Chemistry: Part B 2000;104:237-255.

17. Nguyen T, Kwong RC, Thompson ME, Schwartz BJ. Improving the performance of conjugated polymer-based devices by control of interchain interactions and polymer film morphology. Applied Physics Letters 2000;76:2454-2456.

18. Liu J, Guo TF, Shi Y, Yang Y. Solvation induced morphological effects on the polymer/metal contacts. Journal of Applied Physics 2001;89:3668-3673.

19. Liu J, Shi Y, Yang Y. Solvation-induced morphology effects on the performance of polymer-based photovoltaic devices. Advanced Functional Materials 2001;11:420-424.

20. Liu J, Shi Y, Ma L, Yang Y. Device performance and polymer morphology in polymer light emitting diodes: the control of device electrical properties and metal/polymer contact. Journal of Applied Physics 2000;88:605-609.

21. Yang CY, Hide F, Diaz-Garcia MA, Heeger AJ, Cao Y. Microstructure of thin films of photoluminescent semiconducting polymers. Polymer 1998;39:2299-2304.

22. Cossiello RF, Akcelrud L, Atvars TDZ. Solvent and molecular weight effects on fluorescence emission of MEH-PPV. Journal of the Brazilian Chemical Society 2005;16:74-86.

23. Shi Y, Liu J, Yang Y. Device performance and polymer morphology in polymer light emitting diodes: The control of thin film morphology and device quantum efficiency. Journal of Applied Physics 2000;87:4254-4263.

24. Arnautov SA, Nechvolodova EM, Bakulin AA, Elizarov SG, Khodarev AN, Martyanov DS, Paraschuk DY. Properties of MEH-PPV films prepared by slow solvent evaporation. Synthetic Metals 2004;147:287-291.

25. Kemerink M, van Duren JKJ, Van Breemen AJJM, Wildeman J, Wienk MM, Blom PWM, Schoo HFM, Janssen RAJ. Substitution and preparation effects on the molecular-scale morphology of PPV films. Macromolecules 2005;38:7784-7792.

26. Nguyen T, Schwartz BJ, Schaller RD, Johnson JC, Lee LF, Haber LH, Saykally RJ. Near-field scanning optical microscopy (NSOM) studies of the relationship between interchain interactions, morphology, photodamage, and energy transport in conjugated polymer films. Journal of Physical Chemistry B 2001;105:5153-5160.

27. Nguyen T, Kwong RC, Thompson ME, Schwartz BJ. Improving the performance of conjugated polymer-based devices by control of interchain interactions and polymer film morphology. Applied Physics Letters 2000;76:2454-2456.

28. Liu J, Guo T, Yang Y. Effects of thermal annealing on the performance of polymer light emitting diodes. Journal of Applied Physics 2002;91:1595-1600.

29. Yang Y, Shi Y, Liu J, Guo TF. The control of morphology and the morphological dependence of device electrical and optical properties in polymer electronics. *Electronic and Optical Properties of Conjugated Molecular Systems in Condensed Phases:* Hotta, S., Ichino, Y., Yoshida, Y., (Eds.); Research Signpost: Kerala, India, 2003;37:307-354.

30. Kong F, Zhang SY, Yang CZ, Yuan RK. Interchain excited states in annealed poly[2-methoxy-5-(2'-ethyl-hexyloxy)-p-phenylene vinylene] films. Materials Letters 2006;60:3887-3890.

31. Chou H, Lin K, Fan Y, Wang D. Enhancing quantum efficiency of MEH-PPV through the reduction of chain aggregations by thermal treatments. Journal of Polymer Science Part B: Polymer Physics 2005;43:1705-1711.

32. Holzer W, Penzkofer A, Tillmann H, Horhold H-. Spectroscopic and travelling-wave lasing characteristic of gilch-type and horner-type MEH-PPV. Synthetic Metals 2004;140:155-170.

33. Lampert ZE, Lappi SE, Papanikolas JM, Reynolds CLJ, Aboelfotoh MO. Morphology and chain aggregation dependence of optical gain in thermally annealed films of the conjugated polymer poly[2-methoxy-5-(2-ethylhexyloxy)-p-phenylene vinylene]. Journal of Applied Physics 2013;113:1-9.

34. Cossiello RF, Kowalski E, Rodriques PC, Akcelrud L, Bloise AC, deAzevedo ER, Bonagamba TJ, Atvars TDZ. Photoluminescence and relaxation processes in MEH−PPV. Macromolecules 2005;38:925-932.

35. Gaur U, Wunderlich B. Heat capacity and other thermodynamic properties of linear macromolecules. Journal of Physical Chemistry 1981;10:119-152.

36. Shimadzu Scientific Instruments, Inc. Specific heat capacity manual.

37. Arnautov SA, Nechvolodova EM, Lomakin S, Shchegolikhin A. Photo- and thermal-oxidative stability of novel material for photovoltaics: MEH-PPV/TNF blends. Renewable Energy 2008;33:259-261.

38. Wang H, Tao X, Newton E. Thermal degradation kinetics and lifetime prediction of a luminescent conducting polymer. Polymer International 2004;53:20-26.

39. Saidi MAA, Rahman WAWA, Majid RA. Effect of different solvents on the thermal, IR spectroscopy and morphological properties of solution casted PLA/starch films. Malaysian Journal of Fundamental and Applied Sciences 2014;10:33-36.

40. Burroughes JH, Bradley DDC, Brown AR, Marks RN, Mackay K, Friend RH, Burns PL, Holmes AB. Light-emitting diodes based on conjugated polymers. Nature 1990;347:539-541.

41. Brabec CJ, Sariciftci NS, Hummelen JC. Plastic solar cells. Advanced Functional Materials 2001;11:15-26.

42. Silverstein RM, Webster FX, Kiemle DJ. Spectrometric identification of organic compounds. 7th Ed. ed. New York: John Wiley & Sons, Inc.; 2005.

43. Cumpston BH, Parker ID, Jensen KF. In situ characterization of the oxidative degradation of a polymeric light emitting device. Journal of Applied Physics 1997;81:3716-3720.

44. Voss KF, Foster CM, Smilowitz L, Mihailovi D, Askari S, Srdanov G, Ni Z, Shi S, Heeger AJ, Wudl F. Substitution effects on bipolarons in alkoxy derivatives of poly(1,4-phenylene-vinylene). Physical Review B 1991;43:5109-5118.

45. Wutticharoenmongkol P, Supaphol P, Srikhirin T, Kerdcharoen T, Osotchan T. Electrospinning of Polystyrene/MEH-PPV blends. Journal of Polymer Science: Part B: Polymer Physics 2005;43:1881-1891.

46. Scott JC, Kaufman JH, Brock PJ, DiPietro R, Salem J, Goitia JA. Degradation and failure of MEH-PPV light -emitting diodes. Journal of Applied Physics 1996;79:2745-2751.

47. Ram MK, Sarkar N, Bertoncello P, Sarkar A, Narizzano R, Nicolini C. Fabrication and characterization of MEH-PPV langmuir-schaefer films and their application. Synthetic Metals 2001;122:369-378.

48. Hao XT, McKimmie LJ, Smith TA. Spatial fluorescence inhomogeneities in light-emitting conjugated polymer films. Physical Chemistry Letters 2011;2:1520-1525.

49. Lampert ZE, Reynolds CLJ, Papanikolas JM, Aboelfotoh MO. Controlling morphology and chain aggregation in semiconducting conjugated polymers: The role of solvent on optical gain in MEH-PPV. Journal of Physical Chemistry B 2012;116:12835-12841.